Review Paper

Loaded vibrating quartz sensors

V.M. Mecea
Institute of Isotopic and Molecular Technology, P O Box 700, R-3400 Cluj-Napoca 5 (Romania)

(Received May 28, 1993, accepted September 10, 1993)

Abstract

This paper reviews the original contributions in the development of vibrating quartz sensors, loaded with whatever medium solid, liquid or gas The common feature of such a loading is its ability to vibrate synchronously with the quartz resonator as a compound resonator The paper introduces a new concept in vibrating quartz sensors, where the vibrational characteristics of such a compound resonator, namely the nominal frequency and vibrational amplitude, are correlated to the physical characteristics of the medium vibrating synchronously with the quartz resonator as a compound resonator The energy transfer model is introduced to explain the microweighing capability of quartz resonators Further, it is proved that microweighing is a common feature of all quartz resonators, whatever their vibrational mode It is also proved that other piezoelectric resonators exhibit the same capability Damping of quartz-resonator vibrations at certain temperatures during a temperature sweep is correlated with the deposited film morphology Resonance of the gas within a cavity is used for the development of tunable gas sensors Examples are given for hydrogen and methane detection without using a catalyst An experiment called 'Nanobalance' is also presented, which was performed in outer space

Contents

1. Introduction

Ever since quartz-crystal resonators have been used for frequency-control applications in radiocommunication equipment, the effect of an added mass on their resonance frequency has been known However, the understanding of the mass-induced downwards shift of

the resonance frequency was only of a qualitative nature, and this phenomenon was not carefully investigated until the late 1950s

The possibility of using piezoelectric quartz resonators as quantitative mass-measuring devices was first explored by Sauerbrey [1] The decrease of the resonance frequency of a thickness shear vibrating quartz crystal, having either AT or BT cut, was found to be proportional to the added mass of the deposited film

$$\Delta f = -\frac{f_q^2}{N\rho_q S} M_f \tag{1}$$

where f_q is the fundamental resonance frequency of the quartz, N is the frequency constant of the specific crystal cut (N_{AT} = 1670 kHz mm, N_{BT} = 2500 kHz mm), ρ_q is the quartz density and S is the surface area of the deposited film Introducing the substitution

$$M_q = \frac{N\rho_q S}{f_q} \tag{2}$$

eqn (1) becomes

$$\frac{\Delta f}{f_q} = -\frac{M_f}{M_q} \tag{3}$$

where M_q is the mass of the vibrating quartz

Sauerbrey also revealed that the sensitive area of a thickness shear vibrating quartz resonator is roughly restricted to the electrode area, having its maximum at the centre of the electrode

It was also shown that the shear vibration amplitude on the quartz resonator surfaces closely follows the weighing sensitivity curve [2, 3]

When the film deposited on the quartz resonator surface covers the entire sensitive area, eqns (1) and (3) might be written as follows

$$\Delta f = -\frac{f_q^2}{N\rho_q} m_f \tag{4}$$

or

$$\frac{\Delta f}{f_q} = -\frac{m_f}{m_q} \tag{5}$$

where $m_f = M_f/S$ and $m_q = M_q/S$ are the areal densities of the deposited film and quartz, respectively. Equation (5) is well supported by experimental data [4, 5] up to a mass load m_f/m_q of about 2%

In spite of the fact that eqn (4) or (5), known as the 'frequency measurement technique', is well supported by the experimental data for a small added mass, a sounder justification from a theoretical point of view was needed

Within these efforts, a perturbation analysis was applied by Stockbridge [6] It was assumed that the mass added to an antinode of a vibrating system, such as the surface of a quartz-crystal resonator vibrating in a thickness shear mode, does not store potential energy In other words, acoustic waves do not propagate in the deposited film The result of this analysis is the following equation [7]

$$\frac{\Delta f}{f_q} = \left[\left(1+2\frac{m_f}{m_q}\right)^{-1} - \left(\frac{m_f}{m_q}\right)^2\right]^{1/2} - 1 \tag{6}$$

As the mass of the deposited material becomes appreciable and forms a uniform layer of finite thickness, the assumption that acoustic waves do not propagate in the film becomes less acceptable

In an effort to rectify these difficulties, the quartz–film combination was treated by Miller and Bolef as a composite acoustic resonator [8] The deposited film is considered as an integral part of the vibrating system Thus, contrary to Stockbridge's assumption, an acoustic wave actually propagates into the film Provided that the acoustic losses in the quartz and thin film are small, the calculations could be restricted to the first two terms of the series expansion of the trigonometric functions, finally leading to eqns (4) or (5)

On the other hand, Behrndt [9] has shown that the equation derived by Sauerbrey could be modified, taking into account the frequency f_c of the coated quartz resonator, and proposed the following frequency–mass relationship

$$\Delta f = -\frac{f_q f_c}{N\rho_q} m_f \tag{7}$$

or

$$m_f = \rho_q N\left(\frac{1}{f_c} - \frac{1}{f_q}\right) = \rho_q N\Delta\tau \tag{8}$$

where $\Delta\tau$ is the change of the vibration period of the coated quartz resonator For selected materials eqn (8) is accurate up to a mass load of 10% Its use for microweighing is known as the 'period measurement technique'

On the basis of the composite acoustic resonator model introduced by Miller and Bolef, a more accurate equation was derived by Lu and Lewis [10]

$$\tan\left(\frac{\pi f_c}{f_q}\right) = -\frac{\rho_f v_f}{\rho_q v_q}\tan\left(\frac{\pi f_c}{f_f}\right) \tag{9}$$

where f_c is the compound resonator frequency, f_q is the uncoated quartz resonator frequency, f_f is the mechanical frequency of the deposited film of thickness l_f, given by

$$f_f = \frac{v_f}{2l_f}$$

while ρ_f, ρ_q, v_f and v_q stand for the density and shear-wave velocity of the deposited film and quartz, respectively Equation (9) can also be written in the following form [11]

$$M = \frac{\arctan(Z \tan \pi F)}{\pi Z(1-F)} \tag{10}$$

where $Z = z_q/z_f = \rho_q v_q/\rho_f v_f$ is the ratio of the acoustic impedances, $M = m_f/m_q = \rho_f l_f/\rho_q l_q$ is the ratio of the areal densities and $F = (f_q - f_c)/f_q = -\Delta f/f_q$ is the normalized frequency shift This equation, largely used in thin-film thickness monitoring applications, is known as the 'Z-match technique' It is well supported by the experimental data up to a mass load of 35% [10], or even 70%, as reported by Benes, who developed this physical model and introduced the 'auto Z-match technique' [12]

Beginning in 1980 attention was focused not only on solid deposits on the surface of the shear vibrating quartz-crystal resonators, but also on liquid deposits Kanash and Bastiaans [13] studied the behaviour of the quartz resonator in a flow cell simulating a liquid chromatographic detector, observing changes in the resonance frequency of the quartz when different liquids passed through the cell Glassford [14] studied the response factor of a liquid-coated quartz-crystal resonator Kanazawa and Gordon [15, 16] treated the case of a quartz resonator in which one of its faces is in contact with a viscous liquid of infinite extent The method used treated the resonance phenomenon as arising from the matching of the shear waves in the quartz and in the overlayer to specific boundary conditions Their final result was the following correlation between the measured frequency change and the liquid and quartz characteristics

$$\Delta f = -f_0^{3/2}(\rho_l \eta_l/\pi\rho\mu)^{1/2} \tag{11}$$

where f_0 is the resonance frequency of the uncoated quartz, ρ_l and η_l are the density and absolute viscosity of the liquid deposit, and ρ and μ are the density and shear modulus of quartz ($\rho = 2\,648$ g cm^{-3} and $\mu = 2\,947 \times 10^{11}$ dyne cm^{-2})

It is very interesting to observe that the compound acoustic resonator model was developed for solid deposits on the surface of the quartz-crystal resonators Equation (10), derived from this model, gives excellent results for solid films and has been used in thin-film monitoring devices of the third and fourth generation during the last twenty years However, this model failed in describing the behaviour of quartz resonators in contact with liquids It also failed in explaining the correlation between the sensitivity and vibrational-amplitude distributions on the surface of the shear vibrating quartz

In looking for a general physical model, able to explain more experimental data, a different model was proposed by Mecea and Bucur [17] This was called the 'energy transfer model' (ETM) The aim of this paper is to reveal the main features of this model, emphasizing its generality and the new applications derived from it

2. The energy transfer model

The main idea of the ETM is that the quartz-crystal resonator and the deposited film form a compound resonator The active part of this compound resonator is represented by the quartz resonator itself, while the deposited film vibrates on account of the energy stored in the quartz-resonator vibration

When a film of foreign material is adherently deposited on the quartz-resonator surface, some of the energy stored in the quartz-resonator vibration is transferred to the film This transferred energy is shared between stored and dissipated energy, according to the elastic and dissipative properties of the deposited film

It is assumed that the adherently deposited film on the quartz-resonator surface does not have its own vibrational frequency, as in Miller and Bolef's theoretical model, but vibrates synchronously with the quartz-resonator surface, with a frequency f_c (or angular frequency ω_c) of the compound resonator There is no *a priori* hypothesis about this new vibrational frequency, but it differs from the frequency f_q (or angular frequency ω_q) of the uncoated quartz resonator

2 1 The infinite quartz-crystal resonator

2 1 1 The infinite quartz-crystal resonator coated by a perfectly elastic film

Let us take a cross section of an unloaded thickness vibrating quartz-crystal resonator of thickness l_q As shown in Fig 1, the x-axis is in the nodal plane of vibration

We assume that the quartz resonator consists of an infinite number of elementary mechanical oscillators Their amplitude of vibration along the y-axis is expressed by

$$A(y) = A_{l_q/2} \sin\left(\frac{\pi y}{l_q}\right) = A_0 \sin\left(\frac{\pi y}{l_q}\right) \tag{12}$$

where A_0 is the maximum amplitude of vibration at the quartz-resonator surface

The element of stored vibrational energy of an infinitely small mechanical oscillator of mass dm is [18]

$$dE_q^s = \frac{1}{2}\omega_q A_y^2\, dm = \frac{1}{2}\rho_q \omega_q^2 A_0^2 \sin\left(\frac{\pi y}{l_q}\right) ds\, dy$$

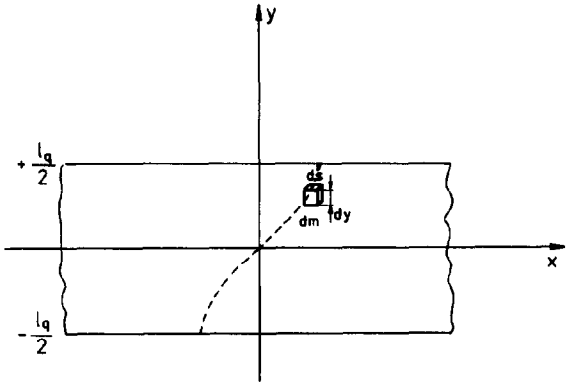

Fig 1 The oscillatory movement of an unloaded thickness shear vibrating quartz-crystal resonator

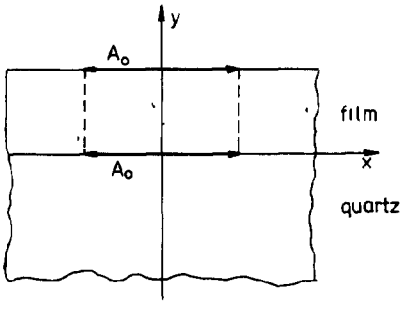

Fig 2 The compound resonator formed by a quartz resonator coated by a perfectly elastic film

Integrating throughout the volume of the quartz resonator, the energy stored by the vibration of an infinite quartz resonator is obtained

$$E_q^s = \frac{1}{4} M_q \omega_q A_0^2 \tag{13}$$

where M_q is the mass of the quartz resonator

When a perfectly elastic film is deposited on the surface of an infinite quartz resonator, the vibrational amplitude of every particle within the deposited film will be identical with that of the uncoated quartz resonator A_0, as illustrated in Fig 2 There will be no vibrational energy dissipated by this perfectly elastic film, so that the following energy balance is established

$$E_q^s = E_{1q}^s + E_f^s \tag{14}$$

where E_q^s is the vibrational energy stored by the uncoated quartz resonator, E_{1q}^s is the remaining vibrational energy stored by the coated quartz resonator, and E_f^s is the vibrational energy stored by the perfectly elastic film In this case, the only vibrational parameter affected by the deposition of a foreign material is the vibrational frequency The new frequency is f_c, or angular frequency ω_c Now, the energy stored by the quartz becomes

$$E_{1q}^s = \frac{1}{4} M_q \omega_c^2 A_0^2 \tag{15}$$

We also assume that the deposited film consists of an infinite number of elementary mechanical oscillators vibrating with the amplitude A_0 The element of stored vibrational energy of an infinitely small mechanical oscillator within the deposited film will be

$$dE_f^s = \frac{1}{2} \rho_f \omega_c^2 A_0^2 \, ds \, dy$$

Integrating throughout the volume of the deposited film, we get the energy stored by the deposited film

$$E_f^s = \frac{1}{2} M_f \omega_c^2 A_0^2 \tag{16}$$

By substituting eqns (13), (15) and (16) into eqn (14) we get

$$\frac{\omega_q^2}{\omega_c^2} = 1 + 2 \frac{M_f}{M_q} \tag{17}$$

or

$$\frac{f_q^2}{f_c^2} = 1 + 2 \frac{M_f}{M_q} \tag{18}$$

In terms of areal densities this equation might be written

$$\frac{f_q^2}{f_c^2} = 1 + 2 \frac{m_f}{m_q} = 1 + 2 \frac{\rho_f l_f}{\rho_q l_q} \tag{19}$$

because $M_f = m_f S$ and $M_q = m_q S$

2 1 2 The infinite quartz-crystal resonator coated by a real film

When the deposited film is a real one, the vibrational energy transferred to it is shared between stored and dissipated energy according to its elastic and inelastic properties

$$E_f^t = E_f^s + E_f^d$$

We admit that both the frequency and vibrational amplitude will change following the deposition of a real film The energy stored in the quartz-crystal vibration after the deposition of such a film will be

$$E_{1q}^s = \frac{1}{4} M_q \omega_c^2 A_{1q} \tag{20}$$

where A_{1q} is the new vibrational amplitude, as shown in Fig 3 In the case of a real film deposited on a quartz-resonator surface, a small slip occurs between the adjacent elementary layers of the film, which gives rise to a frictional force between the adjacent layers

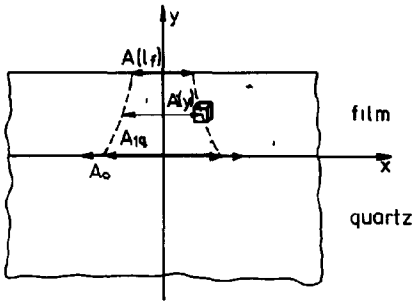

Fig 3 The compound resonator formed by a quartz resonator coated by a real film

The work done by this force gives the energy dissipated within the deposited film A similar approach was taken for the case of liquid deposits on a shear vibrating quartz resonator by Glassford [14]

We can express the vibrational amplitude at each point y of the deposited film, along the ordinate, by an equation given by Landau and Lifschitz [19]·

$$A_f(y)=A_{1q}\exp\left[-\left(\frac{\omega_c}{2\nu_f}\right)^{1/2}y\right]$$

$$=A_{1q}\exp\left[-\left(\frac{\omega_c}{2\nu_f}\right)^{1/2}v_f t\right] \tag{21}$$

where A_{1q} is the vibrational amplitude of the loaded quartz-crystal resonator, $\omega_c=2\pi f_c$ is the angular frequency of the loaded quartz resonator, $\nu_f=\eta_f/\rho_f$ is the kinematic viscosity of the deposited film, given as the ratio of the absolute viscosity to the density of the deposited film, and v_f is the shear-wave velocity in the film

The slip of the y plane relative to the quartz–film interface is

$$\delta_y=A_{1q}-A_f(y)=A_{1q}\left\{1-\exp\left[-\left(\frac{\omega_c}{2\nu_f}\right)^{1/2}y\right]\right\}$$

Thus, the elementary slip between the adjacent layers of the film will be

$$\mathrm{d}\delta_y=A_{1q}\left(\frac{\omega_c}{2\nu_f}\right)^{1/2}\exp\left[-\left(\frac{\omega_c}{2\nu_f}\right)^{1/2}y\right]\mathrm{d}y \tag{22}$$

The frictional force developed in the x–z plane of the film, parallel to the quartz resonator surface, is

$$F_{xz}=S\eta_f\frac{\mathrm{d}U_f}{\mathrm{d}y} \tag{23}$$

where S is the frictional surface and $U_f=\partial A(y)/\partial t$ is the sliding speed of the deposited film particles We obtain

$$F_{xz}=\frac{1}{2}S\rho_f A_{1q}\omega_c v_f\exp\left[-\left(\frac{\omega_c}{2\nu_f}\right)^{1/2}y\right] \tag{24}$$

The element of the dissipated energy between the adjacent layers of the deposited film is

$$\mathrm{d}E_f^d=F_{xz}\,\mathrm{d}\delta_y=\frac{1}{2}S\rho_f A_{1q}^2 v_f\omega_c\left(\frac{\omega_c}{2\nu_f}\right)^{1/2}$$

$$\times\exp\left[-2\left(\frac{\omega_c}{2\nu_f}\right)^{1/2}y\right]\mathrm{d}y \tag{25}$$

The whole vibrational energy dissipated by a film of thickness l_f, deposited on a quartz resonator surface, is

$$E_f^d=\frac{1}{4}S\rho_f A_{1q}^2 v_f\omega_c\left\{1-\exp\left[-2\left(\frac{\omega_c}{2\nu_f}\right)^{1/2}l_f\right]\right\} \tag{26}$$

The vibrational energy stored by an elementary volume of the deposited film is

$$\mathrm{d}E_f^s=\frac{1}{2}\rho_f\omega_c^2A_f^2(y)\,\mathrm{d}s\,\mathrm{d}y$$

$$-\frac{1}{2}\rho_f\omega_c^2A_{1q}^2\exp\left[-2\left(\frac{\omega_c}{2\nu_f}\right)^{1/2}y\right]\mathrm{d}s\,\mathrm{d}y$$

The vibrational energy stored by the whole film is

$$E_f^s=\frac{1}{4}S\rho_f\omega_c^2A_{1q}^2\left(\frac{2\nu_f}{\omega_c}\right)^{1/2}\left\{1-\exp\left[-2\left(\frac{\omega_c}{2\nu_f}\right)^{1/2}l_f\right]\right\} \tag{27}$$

We have already assumed that, following the deposition of a film onto a quartz-resonator surface, the vibrational energy stored by the quartz resonator diminishes from E_q^s to E_{1q}^s, because part of it is transferred to the film We also assume that the energy transferred to the ambient or to the quartz-resonator mounting is very small and will thus be neglected Therefore, the energy balance for the compound resonator will be

$$E_q^s=E_{1q}^s+E_f^s+E_f^d \tag{28}$$

Furthermore, we assume that the decrease of the quartz-resonator vibrational amplitude, at a constant frequency, is a consequence of the vibrational energy dissipated within the deposited film Thus we have

$$\frac{1}{4}M_q\omega_q^2(A_0^2-A_{1q}^2)=\frac{1}{4}S\rho_f\omega_c A_{1q}^2v_f$$

$$\times\left\{1-\exp\left[-2\left(\frac{\omega_c}{2\nu_f}\right)^{1/2}l_f\right]\right\} \tag{29}$$

On substituting eqns (13), (20), (26) and (27) into eqn (28), we obtain

$$\frac{\omega_q^2}{\omega_c^2}=1+2\frac{M_f}{M_q}\left[2\left(\frac{\omega_c}{2\nu_f}\right)^{1/2}l_f\right]^{-1}\left\{1-\exp\left[-2\left(\frac{\omega_c}{2\nu_f}\right)^{1/2}l_f\right]\right\} \tag{30}$$

where M_f is the mass of the deposited film and M_q is that of the quartz In terms of areal densities and frequencies, this equation can be written as

$$\frac{f_q^2}{f_c^2} = 1 + 2\frac{m_f}{m_q}\left[2\left(\frac{\pi f_c}{\nu_f}\right)^{1/2} l_f\right]^{-1}\left\{1 - \exp\left[-2\left(\frac{\pi f_c}{\nu_f}\right)^{1/2} l_f\right]\right\} \tag{31}$$

and gives the correlation between the vibrational frequency of the compound resonator and the mass and kinematic viscosity of the deposited film On developing the exponential function into a power series, we obtain

$$\frac{f_q^2}{f_c^2} = 1 + 2\frac{m_f}{m_q}\left[1 - \left(\frac{\pi f_c}{\nu_f}\right)^{/12} l_f + \frac{2}{3}\left(\frac{\pi f_c}{\nu_f}\right) l_f^2 + \cdots + \frac{(-2)^{n-1}}{n!}\left(\frac{\pi f_c}{\nu_f}\right)^{(n-1)/2} l_f^{n-1}\right]$$

In the case of metallic films, having a very high kinematic viscosity, the series within square brackets reduces to its first term

$$\frac{f_q^2}{f_c^2} = 1 + 2\frac{m_f}{m_q} \tag{32}$$

which is exactly eqn (19) previously derived for the case of perfectly elastic films

If the amount of vibrational energy dissipated within the deposited film is appreciable, we can consider more terms of the power series The effect is a smaller frequency change than for the case of a metallic film, which means a smaller sensitivity

The vibrational amplitude of the uncoated quartz resonator, A_0, as well as that of the compound resonator, A_{1q}, can be measured using the rectified r f voltage, as has been previously proposed [20] The problem of the vibrational-amplitude measurement will be developed in Section 3

2 2 *The finite quartz-crystal resonator*

Actual quartz-crystal resonators have finite dimensions It has been stated that the weighing sensitivity of a thickness shear vibrating quartz-crystal resonator has its maximum value at [1, 21] or close to [5, 22] the centre of the quartz resonator plate, and diminishes towards the edges It was also found that the vibrational amplitude of a plane-parallel quartz resonator has its maximum at [2, 3, 23], or close to [22] the centre of the plate and diminishes towards the edges These experimental data lead to the conclusion that the weighing sensitivity depends on the vibrational amplitude distribution on the surface of the quartz-crystal resonator

This Section of the paper will develop the real case of quartz resonators having finite dimensions and taking into account the amplitude distribution on the surface of a quartz-crystal resonator

Following Sauerbrey's theoretical and experimental work [1–3], we assume that the vibrational-amplitude distribution on the surface of a quartz-crystal resonator obeys the following equation

$$A(r) = A_0 \cos^2\left(\frac{\pi r}{2R_e}\right) \tag{33}$$

where r is the distance from the centre of the plate of a certain point on the quartz-resonator surface, and R_e is the radius of the deposited electrode, assuming that both electrodes have the same diameter, smaller than or equal to the quartz resonator diameter $2R$

In the case of a finite quartz-crystal resonator, the vibrational amplitude of every point within the quartz resonator is defined by

$$A(r, y) = A_0 \sin\left(\frac{\pi y}{l_q}\right)\cos^2\left(\frac{\pi r}{2R_e}\right) \tag{34}$$

where $A_0 = A\ (0, l_q/2)$ is the maximum vibrational amplitude at the surface and centre of the quartz resonator For the sake of convenience, we express the unit volume dv of the quartz in cylindrical coordinates

$$dv = r\ dr\ d\phi\ dy$$

where $0 \leqslant r \leqslant R_e$, $0 \leqslant \phi \leqslant 2$ and $-l_q/2 \leqslant y \leqslant +l_q/2$

The element of stored vibrational energy of an infinitely small mechanical oscillator within the unloaded quartz-crystal resonator will be

$$dE_{qR}^s = \frac{1}{2}\rho_q \omega_q^2 A_0^2 \sin\left(\frac{\pi y}{l_q}\right)\cos^4\left(\frac{\pi r}{2R_e}\right) r\ dr\ d\phi\ dy$$

Integrating throughout the quartz-resonator vibrating volume, we obtain the stored vibrational energy

$$E_{qR}^s = \frac{1}{2}\rho_q l_q \omega_q^2 A_0^2 \pi R_e^2\left(\frac{3}{16} - \frac{1}{\pi^2}\right) \tag{35}$$

2 2 1 *The finite quartz-crystal resonator coated by a perfectly elastic film*

Following the deposition of a perfectly elastic film on the surface of a finite quartz resonator, the energy stored in the quartz-resonator vibration will diminish to a new value expressed by

$$E_{1qR}^s = \frac{1}{2}\rho_q l_q \omega_c^2 A_0^2 \pi R_e^2\left(\frac{3}{16} - \frac{1}{\pi^2}\right) \tag{36}$$

The quartz-resonator vibrational amplitude will remain unchanged throughout the deposited film thickness, as shown in Fig 2, but obeying the surface distribution law expressed by eqn (34) No vibrational

energy will be dissipated by such an ideal film In this case, the element of stored energy in the film will be

$$dE^{s}_{fR}=\frac{1}{2}\rho_f\omega_c^2A_0^2\cos^4\left(\frac{\pi r}{2R_e}\right)r\,dr\,d\phi\,dy$$

Integrating throughout the deposited film, of thickness l_f and radius r_0, centred on the electrode surface, the total vibrational energy stored by the deposited film will be

$$E^{s}_{fR}=\rho_f l_f\omega_c^2A_0^2\pi\left\{\frac{r_0R_e}{4\pi}\sin\left(\pi\frac{r_0}{R_e}\right)\cos^2\left(\frac{\pi}{2}\frac{r_0}{R_e}\right)+\frac{3}{16}r_0^2+\frac{3r_0R_e}{8\pi}\sin\left(\pi\frac{r_0}{R_e}\right)+\frac{R_e^2}{4\pi^2}\left[\cos^4\left(\frac{\pi}{2}\frac{r_0}{R_e}\right)-1\right]+\frac{3R_e^2}{8\pi^2}\left[\cos\left(\pi\frac{r_0}{R_e}\right)-1\right]\right\} \quad (37)$$

If the deposited film covers the whole vibrating area of the quartz resonator, i e , $r_0=R_e$, the vibrational energy stored by the deposited film will be

$$E^{s}_{fR}=\rho_f l_f\omega_c^2A_0^2\pi R_e^2\left(\frac{3}{16}-\frac{1}{\pi^2}\right) \quad (38)$$

In such a case, when no vibrational energy is dissipated by the film covering the whole vibrating area of a finite quartz-crystal resonator, the energy balance indicated by eqn (14) will give

$$\frac{f_q^2}{f_c^2}=1+2\frac{\rho_f l_f}{\rho_q l_q}=1+2\frac{m_f}{m_q} \quad (39)$$

2 2 2 The finite quartz-crystal resonator coated by a real film

In the case of a real film deposited on the surface of a quartz-crystal resonator with finite dimensions, the vibrational amplitude of the deposited film particles will depend not only on the distance from the centre of the quartz-crystal plate, but also on the distance from the quartz-resonator surface The vibrational energy will be dissipated within the deposited film due to the slip of the adjacent layers of the film, as illustrated in Fig 3 The vibrational amplitude of a point within the deposited film may be expressed as

$$A_f(r,y)=A_{1q}\cos^2\left(\frac{\pi r}{2R_e}\right)\exp\left[-\left(\frac{\omega_c}{2\nu_f}\right)^{1/2}y\right] \quad (40)$$

The element of stored vibrational energy within the film will be

$$dE^{s}_{fR}=\frac{1}{2}\rho_f\omega_c^2A_{1q}^2\cos^4\left(\frac{\pi r}{2R_e}\right)\times\exp\left[-2\left(\frac{\omega_c}{2\nu_f}\right)^{1/2}y\right]r\,dr\,d\phi\,dy$$

The vibrational energy stored by a film of thickness l_f covering the whole vibrating area of a quartz resonator of diameter equal to $2R_e$ is

$$E^{s}_{fR}=\frac{1}{2}\rho_f l_f\omega_c^2A_{1q}^2\pi R_e^2\left(\frac{3}{16}-\frac{1}{\pi^2}\right)\left(\frac{2\nu_f}{\omega_c}\right)^{1/2}\times\left\{1-\exp\left[-2\left(\frac{\omega_c}{2\nu_f}\right)^{1/2}l_f\right]\right\} \quad (41)$$

Following the calculation procedure developed in Section 2 1 2, the element of vibrational energy dissipated within the deposited film will be

$$dE^{d}_{fR}=\frac{1}{2}\rho_f\omega_c\nu_fA_{1q}^2\cos^4\left(\frac{\pi r}{2R_e}\right)\left(\frac{\omega_c}{2\nu_f}\right)^{1/2}\times\exp\left[-2\left(\frac{\omega_c}{2\nu_f}\right)^{1/2}y\right]r\,dr\,d\phi\,dy$$

The vibrational energy dissipated by the whole film of thickness l_f and diameter $2R_e$ is

$$E^{d}_{fR}=\frac{1}{2}\rho_f\omega_c\nu_fA_{1q}^2\pi R_e^2\left(\frac{3}{16}-\frac{1}{\pi^2}\right)\times\left\{-\exp\left[-2\left(\frac{\omega_c}{2\nu_f}\right)^{1/2}l_f\right]\right\} \quad (42)$$

The vibrational energy stored by an uncoated quartz-crystal resonator with finite dimensions was given by eqn (35) When this resonator is covered by a real film, the remaining stored vibrational energy will be

$$E^{s}_{1qR}=\frac{1}{2}\rho_q l_q\omega_c^2A_{1q}^2\pi R_e^2\left(\frac{3}{16}-\frac{1}{\pi^2}\right) \quad (43)$$

The energy transfer model supposes that the vibrational energy dissipated within the film induces a decrease of the vibrational amplitude of the compound resonator at a constant frequency Thus the following equation is established

$$\frac{1}{2}\rho_q l_q\omega_q^2\pi R_e^2\left(\frac{3}{16}-\frac{1}{\pi^2}\right)\left(A_0^2-A_{1q}^2\right)=\frac{1}{2}\rho_f\omega_c\nu_fA_{1q}^2\pi R_e^2\left(\frac{3}{16}-\frac{1}{\pi^2}\right)\times\left\{1-\exp\left[-2\left(\frac{\omega_c}{2\nu_f}\right)^{1/2}l_f\right]\right\} \quad (44)$$

The energy balance expressed by eqn (28) will give

$$\frac{\omega_q^2}{\omega_c^2} = 1 + 2\frac{\rho_f l_f}{\rho_q l_q}\left[2\left(\frac{\omega_c}{2\nu_f}\right)^{1/2} l_f\right]^{-1} \times\left\{1 - \exp\left[-2\left(\frac{\omega_c}{2\nu_f}\right)^{1/2} l_f\right]\right\} \quad (45)$$

or, in terms of measured frequency and areal densities, it can be written

$$\frac{f_q^2}{f_c^2} = 1 + 2\frac{m_f}{m_q}\left[2\left(\frac{\pi f_c}{\nu_f}\right)^{1/2} l_f\right]^{-1} \times\left\{1 - \exp\left[-2\left(\frac{\pi f_c}{\nu_f}\right)^{1/2} l_f\right]\right\} \quad (46)$$

It is very important to observe that eqn (46) is identical to eqn. (31) corresponding to an infinite quartz-crystal resonator This is because we made an important assumption that the deposited film covers the whole vibrating area of the quartz resonator, having the diameter $2R_e$ This also leads to a very important conclusion that, in order to have the theoretical sensitivity to the mass of a deposited film, the film must cover the entire vibrating area of the quartz-crystal resonator This important condition was proved experimentally [22] and is revealed in Section 3 of this paper

For the case of thin films with very high kinematic viscosity, like metallic ones, eqn (46) reduces to a simpler form

$$\frac{f_q^2}{f_c^2} = 1 + 2\frac{m_f}{m_q} \quad (47)$$

This equation meets the requirements for thin-film monitoring devices, as will be revealed in the next Section This equation permits the calculation of a deposited film thickness by measuring the frequencies of the quartz-crystal resonator during the coating process, using the following equation

$$l_f = \frac{1}{f_q}\left(\frac{f_q^2}{f_c^2} - 1\right)\frac{N}{2}\frac{\rho_q}{\rho_f} \quad (48)$$

where f_q is the nominal frequency of the quartz resonator before the deposition and f_c is the nominal frequency of the quartz resonator following the deposition of a film having density ρ_f and thickness l_f

2 3 A comparison of the available theoretical approaches

In order to facilitate a comparison of the various theoretical approaches presented in the first Section of this paper with the energy transfer model, the dimensionless parameters M and F, introduced in the first Section, will be used Thus, the following equations will be used instead of those already mentioned

(a) Frequency measurement technique, described by eqn (5)

$$M = F \quad (49)$$

(b) Stockbridge's theoretical model, described by eqn (6)

$$F = 1 - \left(\frac{1}{1+2M} - M^2\right)^{1/2} \quad (50)$$

(c) Period measurement technique, described by eqn (7)

$$F = \frac{M}{1+M} \quad \text{or} \quad M = \frac{F}{1-F} \quad (51)$$

(d) Z-match technique, same as eqn (10)

$$M = \frac{\arctan(Z\tan\pi F)}{\pi Z(1-F)} \quad (52)$$

(e) Energy transfer model, described by eqn (47)

$$F = 1 - (1+2M)^{-1/2} \quad (53)$$

or

$$M = \frac{1}{2}\left[\frac{1}{(1-F)^2} - 1\right] \quad (54)$$

A graphical illustration of these theoretical approaches is presented in Fig 4 This reveals that for small normalized frequency shifts (less than 2%), all the graphical illustrations are superposed The difference becomes more evident as these normalized frequency shifts are increased

The frequency measurement technique is based on the assumption that a foreign film deposited on a quartz-crystal resonator surface induces the same downward frequency shift as an additional layer of quartz having the same mass However, the physical properties of the deposited film might be quite different from those of quartz, and this assumption leads to a limited range of validity of this physical model, namely to very thin metallic depositions

Stockbridge's theoretical model, although more rigorous, did not find practical use, since the higher-order terms require experimentally measured constants with no direct physical interpretation Moreover, eqn (50) has a serious mathematical limitation, since the square root is applied to an amount that is positive only for $M < 0\,65729$ to produce real solutions

The period measurement technique had no other theoretical justification, but is better suited to experimental data in a wider range of relative mass loads M

The Z-match technique represented major progress in quartz-crystal microbalance technique, revealing the influence of the physical properties of the deposited

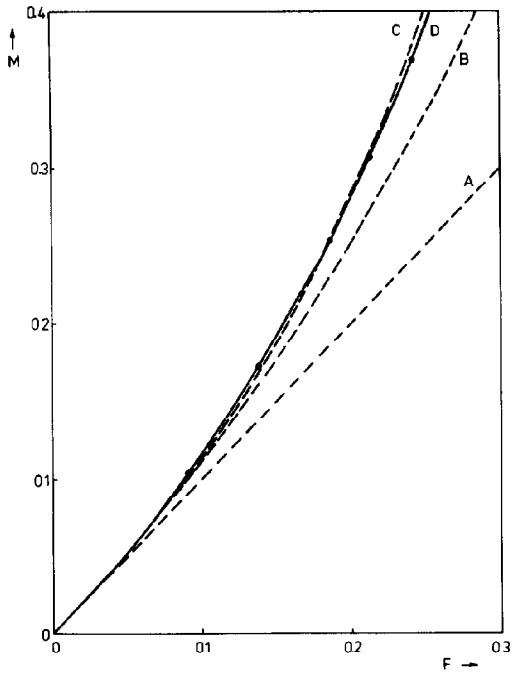

Fig 4 A graphical plot of the reduced mass M as a function of the reduced frequency F for different theoretical approaches A, eqn (49), B, eqn (51), C, eqn (52), D, eqn (54) Dots correspond to gravimetric measurements for copper depositions on a 6 228 MHz BT-cut resonator in vacuum.

film on the frequency change of a thickness shear vibrating quartz-crystal resonator, following the deposition of a film of a foreign material on its surface

One drawback of this technique is the need for the knowledge of the acoustic impedance ratio Z This problem has been circumvented by Benes [12], using Z determination from two quasiharmonic frequencies There are also some questionable aspects of this theoretical model One aspect refers to the mechanical frequency of the deposited film (see eqn (9)) defined by

$$f_f = v_f/2l_f$$

In the initial stages of film condensation on a substrate, the film is rather discontinuous, and we cannot define a certain thickness l_f The expected behaviour would be a sudden frequency decrease as soon as the deposited film becomes continuous Experimentally, a measurable frequency decrease is recorded long before a monatomic film is condensed onto the quartz (electrode) substrate On the other hand, a uniform monatomic film would induce a mechanical shear vibration frequency of about 10^{13} Hz, while the substrate vibrational frequency is in the MHz range From the adherence point of view, this situation cannot be accepted The other aspect refers to another idea of the Z-match technique It states that the free surfaces of a compound resonator are always antinodal [12] This means that the vibrational amplitude at the quartz–film interface is smaller than that corresponding to the free surface of the deposited film Assuming that we have a quartz resonator coated on one side with a dielectric film, the quartz strain at the quartz–film interface will be smaller than its strain at the free surface This means, thinking of the piezoelectric effect, that the electric charge accumulated at a certain moment by the dielectric-coated electrode of the quartz resonator is smaller than the charge of the reverse polarity accumulated by the uncoated electrode This is impossible from a piezoelectric point of view, because the quartz resonator must always be neutral as a whole

It is interesting to observe that the two mentioned inconsistencies, from a physical point of view, lead to a mathematical inconsistency of the Z-match technique Let us look at eqn (10) or (51) When Z differs from unity, the normalized frequency shift F must be less than 1/2 For $F=1/2$ we have $\tan \pi/2 \rightarrow \infty$, and for F higher than 1/2 the relative mass load M becomes negative, which is impossible

Neither of the above-mentioned theoretical approaches, excepting the energy transfer model, can explain the correlation between the mass sensitivity of the shear vibrating quartz resonators and the vibrational-amplitude distribution on their surface This will be seen in Section 3

None of the above-mentioned theoretical approaches, excepting the energy transfer model, can describe the behaviour of shear vibrating quartz resonators in contact with a liquid This will be seen in Section 2 5

It is also interesting to observe that Horvath and Arany [24] independently took an energetic approach similar to that of the energy transfer model, deriving the following equation

$$\frac{\alpha_\Delta}{\alpha} = \left(1+2\frac{\Delta m}{m_q}\right)^{-1/2} \tag{55}$$

where α_Δ is the vibrational frequency of the compound resonator (f_c in our notation), α is the vibrational frequency of the uncoated quartz resonator (f_q in our notation) and Δm is the areal density of the deposited film (m_f in our notation) Equation (55) is identical to eqn (47) that we derived from the energy transfer model Further, Horvath and Arany developed their equation into a McLaurin series, retaining only the first term of this series They obtained

$$\frac{\Delta\alpha}{\Delta m} = -\frac{\alpha}{m_Q} \tag{56}$$

where $\Delta\alpha$ is the frequency change and m_Q is the areal density of the quartz This equation is identical to the

equation derived by Sauerbrey They concluded that Sauerbrey's equation can be obtained following an energetic approach, without realizing that eqn (55), initially obtained, is very accurate, while eqn (56) is only an approximation

2 4 Experimental verification of the mass response of a coated quartz-crystal resonator

When the thickness of the film deposited onto the quartz-resonator surface is very small, so that the relative frequency shift F is less than 0 05, all the theoretical approaches reviewed in the previous Section give excellent results For higher relative frequency shifts, the differences between various theoretical approaches are more evident, as can be seen in Fig 4

In order to verify which theoretical approach suits the experimental results better, it is compulsory to coat the quartz resonator with thicker films Here a new problem appears The thicker the deposited film, the higher the lateral stress developed at the quartz–film interface [25]. This lateral stress causes the deposited film to peel off from the quartz surface, the dissipation of an appreciable amount of vibrational energy at the quartz–film interface, followed by the ceasing of the quartz-resonator vibration In order to overcome this problem, we used quartz resonators with gold/chromium electrodes, taking advantage of the very high adherence of chromium to the quartz surface The thickness of the chromium underlayer was 500 Å, while the gold film had a thickness of 1500 Å Chromium and gold were consecutively vacuum deposited during the same evacuation cycle

Copper was chosen as the deposition material, because it can be easily evaporated and is cheap A laboratory vacuum-deposition unit, model B 30 2 (VEB Hochvakuum Dresden), was used A shear vibrating BT-cut quartz-crystal resonator with a fundamental resonance frequency of 6 228 MHz was used It had a plano-convex plane shape and a 14 mm diameter Every deposition was followed by a frequency shift The relative frequency shifts F were used to calculate the relative areal densities M for consecutive depositions Calculations were performed for the widely used theoretical approaches, using the following equations

eqn (49) for the frequency measurement technique
eqn (51) for the period measurement technique
eqn (52) for the Z-match technique
eqn (54) for the energy transfer model

The areal density of the quartz, m_q, was calculated starting from the fundamental vibrational frequency of the uncoated quartz resonator Thus we have

$$m_q = \rho_q l_q = \rho_q \frac{N}{f_q} \tag{57}$$

This is, in fact, an equivalent areal density, corresponding to the vibrating part of the quartz resonator

The deposition diameter, resulting from the measuring head aperture, was 8 mm, thus covering the whole sensitive area of the quartz resonator This area was previously explored using the method that will be described in Section 3

Gravimetric measurements of the copper depositions were performed with a Sartorius model 2406 analytical microbalance The results are shown in Table 1 For the sake of simplicity, only the relative errors are recorded when the indicated equations were used

The results shown in Table 1 prove that eqn (54) derived from the energy transfer model for solid films fits the gravimetric measurements best This is also illustrated in Fig 4, where the dots corresponding to the direct gravimetric measurements give the best fit to the graphical representation of eqn (54)

Although the relative errors given by eqn (52) derived from the Z-match technique are rather small, this is not a sufficient proof of validity of the model, because this model cannot explain the correlation between the mass sensitivity and vibrational-amplitude distribution on the quartz-resonator surface and cannot describe the response of a quartz resonator in contact with a liquid

The very large relative errors exhibited by the frequency measurement and period measurement techniques limit their usable range In order to get relative errors less than 1%, the relative frequency shifts should be smaller than 0 67% for the frequency measurement technique, or smaller than 1 98% for the period measurement technique

2 5 Frequency response of a quartz resonator in contact with a liquid

When a quartz-crystal resonator is coated by a liquid film, which has a much lower viscosity (about 10^{-2} P) than that corresponding to a metallic film (about 10^{15} P), the general eqn (46), derived from the energy transfer model, must be taken into account

Introducing the substitutions

$$f_q = \frac{1}{2l_q}\left(\frac{\mu_q}{\rho_q}\right)^{1/2} \quad \text{and} \quad \nu_f = \frac{\eta_f}{\rho_f}$$

where μ_q is the shear modulus of quartz ($\mu_q = 2\,947 \times 10^{11}$ dyne cm^{-2}) and ν_f is the kinematic viscosity of the liquid film, we obtain

$$\Delta f = -f_q^{3/2}\left(\frac{\rho_f \eta_f}{\pi \rho_q \mu_q}\right)^{1/2} \times \left\{1 - \exp\left[-2\left(\frac{\pi f_c \rho_f}{\eta_f}\right)^{1/2} l_f\right]\right\} \frac{2f_c^2}{(f_q + f_c)(f_q f_c)^{1/2}}$$

TABLE 1 Relative errors resulting from the use of various equations, when compared with gravimetric measurements of copper deposits, for different relative frequency shifts

		Gravimetric	Eqn (49) (%)	Eqn (51) (%)	Eqn (52) (%)	Eqn (54) (%)
F	M	l_f (μm)				
0 048	0 052	6 17	−7 5	−2 9	−2 2	−0 49
0 092	0 107	12 77	−14 1	−5 4	−3 2	−0 53
0 139	0 174	20 77	−19 8	−6 8	−1 8	−0 66
0 186	0 253	30 21	−26 3	−10 5	−0 26	−0 85
0 213	0 305	36 51	−30 1	−11 2	+1 1	−0 84
0 243	0 370	44 22	−34 3	−13 3	+2 8	−0 53

This is exactly eqn (11) derived by Kanazawa and Gordon [15] multiplied by two additional factors It is important to evaluate the magnitude of these additional factors One can observe that the exponent contains the reciprocal of the characteristic decay length δ [19]

$$\delta = \left(\frac{\eta_f}{\pi f_c \rho_f}\right)^{1/2} \tag{58}$$

The characteristic decay length is the thickness of the liquid layer, in contact with a solid vibrating surface, across which the vibrational amplitude diminishes e times This can be seen in Fig 5, which also reveals that the thickness of the vibrating liquid layer is larger than the characteristic decay length δ, thus concluding that the magnitude of the first factor is equal to unity

$$1-\exp\left[-2\left(\frac{l_f}{\delta}\right)\right]=1$$

In order to evaluate the magnitude of the second additional factor, we can consider the experimental results obtained by Kanazawa and Gordon [15] Using a 5 MHz AT-cut quartz resonator, they obtained frequency shifts of about 500 Hz for glucose–water mixtures Using these numerical data we get the value 0 9999 for the second factor, which is close to unity This is a proof that the equation derived by Kanazawa and Gordon [15] can also be obtained starting from the energy transfer model This model has a high degree of generality covering the frequency response of coated quartz resonators with various layers whose viscosity covers 17 orders of magnitude

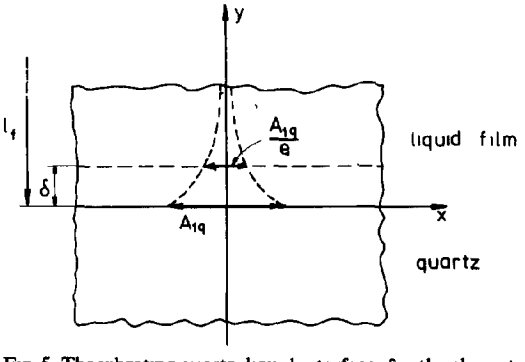

Fig 5 The vibrating quartz–liquid interface δ is the characteristic decay thickness

2 6 *Damping of the quartz-crystal resonator vibrations in contact with a liquid*

When a quartz resonator is coated with a liquid film, not only the frequency of the compound resonator changes, but also its vibrational amplitude If the amount of energy supplied to the liquid-coated quartz resonator is small, its vibration will cease because of the important amount of energy dissipated within the liquid film With modern existing electronics, it is possible to supply sufficient energy to the compound resonator to sustain its oscillation

Mecea and Bucur [20] showed that the damping of the quartz-crystal resonator vibrations depends on the viscosity of the layer deposited on the quartz-resonator surface They used the rectified r f voltage U to record this behaviour U is a d c voltage proportional to the coated quartz-resonator vibrational amplitude, provided that no distortion of the sine-wave output is introduced by the electronic circuitry Because of the piezoelectric effect, there is always a proportionality between the voltage across the electrodes and the strain [12] Thus we have

$$V=\frac{e}{\epsilon}\left[1-\cos\left(\frac{\pi f_c}{f_q}\right)\right]A_{1q} \tag{59}$$

where V is the sine voltage across the quartz-resonator electrodes, e is the piezoelectric constant and ϵ is the quartz permittivity In the case of a fixed load, there is a direct proportionality between the high-frequency voltage V and the corresponding rectified voltage U

$$U=kV=k^*A_{1q} \tag{60}$$

By recording U we have an indication of the quartz-crystal resonator vibrational amplitude

An experiment was carried out using a BT-cut quartz resonator with a nominal frequency of 4 4826 MHz

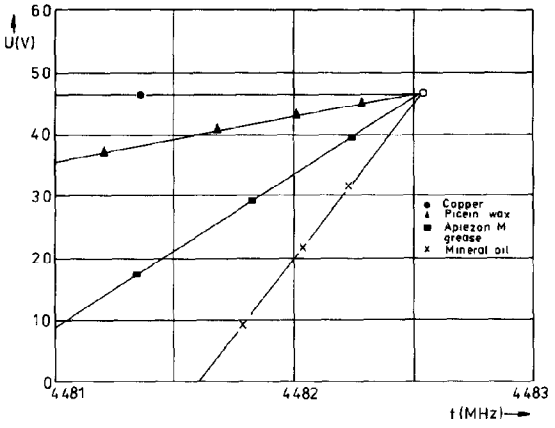

Fig 6 Damping of the quartz-resonator vibrations when coated with layers of different viscosities

This was subsequently coated with various layers copper, picein wax, Apiezon M grease and mineral oil With copper deposition there was no change in the recorded voltage U The lower the coating viscosity, the more important was the decrease of the recorded voltage U, corresponding to the vibrational amplitude of the compound resonator This is illustrated in Fig 6 The experiments were carried out at room temperature

3. Mass sensitivity and amplitude-distribution measurements on the surface of the quartz resonators

It has been demonstrated by Sauerbrey [1] that the local mass sensitivity of a shear vibrating quartz-crystal resonator depends on the local vibrational amplitude

Through the years, various methods of measuring the vibration amplitude of the quartz resonators have been developed The best results were obtained by the modulation of a light beam [2] and by the speckle effect [23]

In looking for a simple mechanical set-up, insensitive to environmental disturbances, a very simple method has been developed [22]

The working principle of this method is based on the energy transfer method Here it is supposed that no vibrational energy is dissipated within the quartz-crystal electrodes, but some might be dissipated by a frictional force, developed by a small soft tip resting under gravity on selected points on the surface of the quartz-crystal resonator This dissipated energy is expressed by

$$E^{d} = \mu F_n A_0 \cos^2\left(\frac{\pi r}{2R_e}\right) \tag{61}$$

where μ is the frictional coefficient at the quartz (electrode)–tip interface, F_n is the weight of the tip–wire assembly and $A(r)=A_0 \cos^2(\pi r/2R_e)$ is supposed to be the amplitude distribution on the quartz-resonator surface, covered on both sides with electrodes of diameter $2R_e$ [3] Assuming that the frictional coefficient and the weight of the tip–wire assembly are constant, and the tip is moved slowly at constant speed across the quartz-resonator diameter, then the energy-dissipation curve will follow the vibration-amplitude distribution on the quartz-resonator surface

The experimental arrangement is shown schematically in Fig 7 The quartz-crystal resonator is mounted horizontally on a sliding system, controlled by a micrometer gauge The tip–wire assembly is laid freely on the quartz-resonator surface under its own weight $F_n = 2\times10^{-3}$ N It is driven across the quartz-resonator diameter at a constant speed of 1×10^{-5} m s^{-1} by means of a small low-geared synchronous a c motor

The quartz-resonator electrodes are connected to the amplitude-controlled oscillator, driven by the quartz resonator itself The r f voltage between the quartz electrodes remains constant at about 30 mV peak-to-peak, within a wide range of vibration-energy dissipation at the quartz–tip interface The discrete transistor works as a series voltage regulator The voltage between the points A and B varies between 0 9 V for high-quality quartz resonators and 10 V for strongly damped resonators The voltage between points A and B and also the voltage drop across the resistor R will, when the soft tip is moving towards higher vibration-amplitude points on the quartz-resonator surface, increase in line with the increased frictional loss The magnitude of this voltage is recorded graphically

In order to check that the vibrational energy dissipation profile can be an indication of the mass-sensitivity distribution on the surface of a thickness shear vibrating quartz resonator, mass-loading experiments were also performed For checking the mass-sensitivity profile on the surface of the quartz resonators, a pair of quartz thin-film thickness-measuring heads was used One of these heads was modified in order to facilitate the deposition of thin films as small spots at certain points across a diameter of the quartz res-

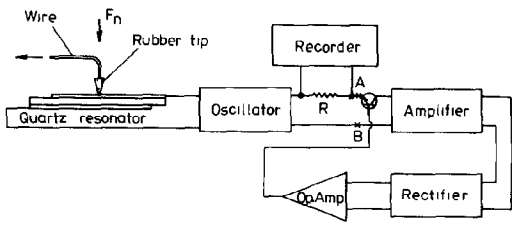

Fig 7 Schematic diagram of the apparatus for measuring the amplitude distribution on the quartz-resonator surface

onator This head had a sliding shutter with a small aperture, set in position by a motorized micrometer gauge

Two different types of quartz-crystal resonators were examined The first was a conventional plane-parallel, 5 MHz AT-cut quartz-crystal resonator with bevelled edges and 14 mm diameter It had 6 mm vapour-deposited silver-film electrodes on both sides The second was a plano-convex 5 MHz At-cut quartz resonator of 14 mm diameter and 200 mm curvature radius It had vapour-deposited silver-film electrodes of different diameters on each side 13 mm on the flat side and 6 mm on the curved side

An indication of the vibration energy dissipated at the quartz–tip interface was obtained by recording the voltage drop U across the resistor R for each quartz resonator

Every quartz resonator was subsequently mounted in the assembly with the sliding aperture and placed in a vacuum deposition unit, using the adjacent thickness-measuring head as a control Equally spaced silver-film spots of constant area and thickness were deposited along the diameter of each quartz resonator previously explored for amplitude distribution Figure 8 shows (full curve) the recorded voltage drop U across the resistor R, as an indication of the amplitude distribution on the plane-parallel quartz-resonator surface The mass-sensitivity curve is drawn (broken curve) by recording the frequency decrease $\Delta F = f_q - f_c$, for every equal silver film spot These spots were of 1 2 mm diameter with a spacing of 1 mm The results illustrated in Fig 8 show that, for plane-parallel quartz-crystal resonators

(a) the frequency sensitivity of the resonator to mass loading of the surface closely follows the vibration amplitude distribution,

(b) the mass-sensitive area is larger than the electrode area,

(c) the maximum of the mass sensitivity and vibration amplitude is off-centre

Figure 9 shows a similar record for a plano-convex quartz crystal resonator Here the spots were of 0 6 mm in diameter and 0 5 mm spacing The results illustrated in Fig 9 show that, for plano-convex quartz-crystal resonators

(a) the frequency sensitivity of the resonator to mass loading of the surface closely follows the vibration amplitude distribution,

(b) the mass-sensitive area is restricted to the smaller of the two electrode areas,

(c) the maximum mass sensitivity is at the centre of the quartz-crystal resonator

The apparent connection between the mass sensitivity of the quartz-crystal resonators and the vibration-amplitude distribution, shown in Figs 8 and 9, can be explain within the energy transfer model This model states that, following a thin-film deposition, the frequency shift is induced by the vibration energy transferred to the film as a stored energy, which is expressed by the following equation

$$E_f^s = \frac{1}{2} M_f \omega_c^2 A^2(r)$$

where M_f is the mass of the deposited film, ω_c is the angular frequency of the compound resonator thus formed and $A(r)$ is the vibration amplitude at the point where the deposited film spot is located This equation states that for equal depositions the energy transferred to the film as a stored energy, and hence the frequency shift, will be higher when the vibration amplitude is higher

The sensitive area of the plane-parallel quartz-crystal resonators extends beyond the whole electrode area

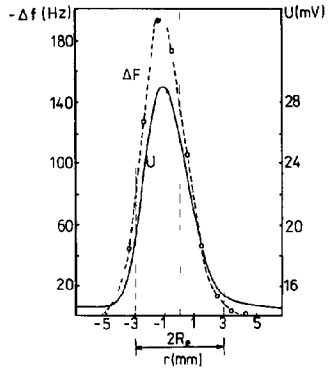

Fig 8 Correlation of the vibration amplitude change ΔU and frequency change Δf corresponding to identical silver spot depositions on the surface of a plane-parallel, AT-cut, 5 MHz quartz-crystal resonator

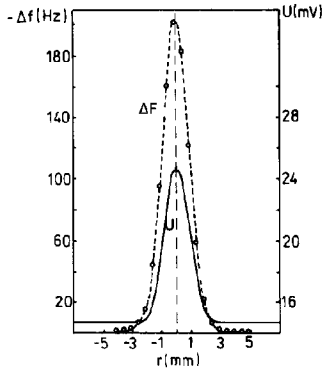

Fig 9 Correlation of the vibration amplitude change ΔU and frequency change Δf corresponding to identical silver spot depositions on the surface of a plano-convex, AT-cut, 5 MHz quartz-crystal resonator

and the maximum of the sensitivity is asymmetric Such an asymmetry was also found by Mueller and White [5] It has not been explained, but might be caused by a dimensional non-uniformity, for example, in the quartz plate thickness

The sensitive area of the plano-convex quartz resonators is restricted to the electrode area and these resonators are therefore more suitable for use in the measurement of the thin-film thickness

4. Microweighing with quartz resonators having other vibrational modes

When treating the case of quartz-resonator mass sensors, the up-to-date literature refers only to shear vibrating quartz resonators, mainly AT-cut and seldom BT-cut resonators

One could certainly ask if the microweighing capability is exhibited only by the thickness shear vibrating quartz resonators To answer this question, some experiments were carried out to check whether quartz resonators having other vibrational modes are also sensitive to an added mass

First an X-cut quartz resonator was tested This vibrates in a compressional mode, generating ultrasonic longitudinal waves in air, as shown in Fig 10 A 1 MHz resonator, in the form of a disc with 20 mm diameter and 2 87 mm thickness was used Its median plane is a nodal plane, while both surfaces are antinodal The vibration amplitude of every point within this resonator can be described by

$$A_y = A_0 \sin\left(\frac{\pi y}{l_q}\right) \tag{62}$$

where A_0 is the maximum vibration amplitude at the antinodal surfaces and l_q is the quartz-resonator thickness This equation is identical to that of the shear vibrating quartz resonators used in Section 2 The calculations, within the energy transfer model, will give the following result for the case of perfectly elastic films

$$\frac{f_q^2}{f_c^2} = 1 + 2\frac{m_f}{m_q} \tag{63}$$

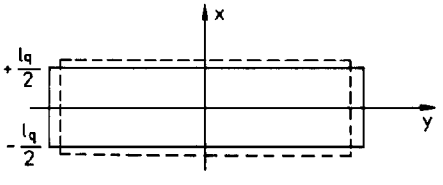

Fig 10 Schematic drawing of the X-cut quartz resonator vibrating in a compressional mode

As can be seen from Fig 10, the entire surface of this resonator is antinodal For this reason, depositions were carried out on the entire surface of the X-cut resonator Silver films were vacuum deposited onto one surface of this resonator Following each deposition, a frequency change was measured and the mass of the silver deposition was measured using a Sartorius microbalance (model 2406) The results are shown in Fig 11 The solid line is the plot of eqn (63) and the dots are experimental points It is very clear that such a resonator is sensitive to the mass of a deposited film and the experimental points fit the same equation as in the case of shear vibrating quartz resonators

Further, a CT-cut quartz resonator vibrating in a face-shear mode was checked The vibration of such a resonator is illustrated in Fig 12 There is no antinodal surface The vibration amplitude varies from zero to the maximum value on each of the two major surfaces of the resonator Silver films were deposited onto one of these major surfaces of a 357 3 kHz CT-cut quartz resonator The experimental results are shown in Fig 13 This kind of resonator is also sensitive to the mass of the deposited films The experimental points do not fit the solid line corresponding to eqn (63) This is because the deposited silver films do not cover an entirely antinodal surface as in the case of the quartz

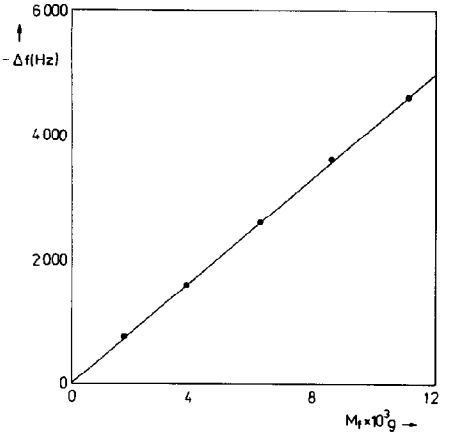

Fig 11 Frequency response of a 1 MHz X-cut quartz resonator coated by a silver film

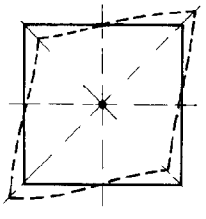

Fig 12 Schematic drawing of a CT-cut quartz resonator vibrating in a face-shear mode

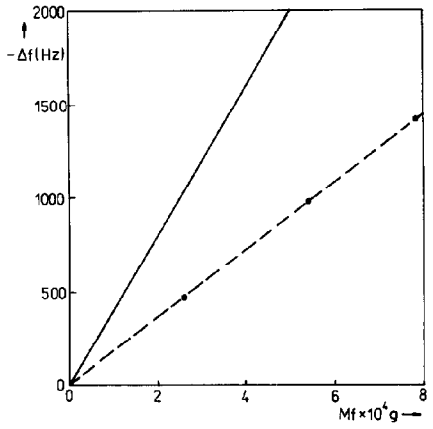

Fig 13 Frequency response of a 357 3 kHz CT-cut quartz resonator coated by silver films Solid line corresponds to eqn (53), while the broken line corresponds to the experimental results

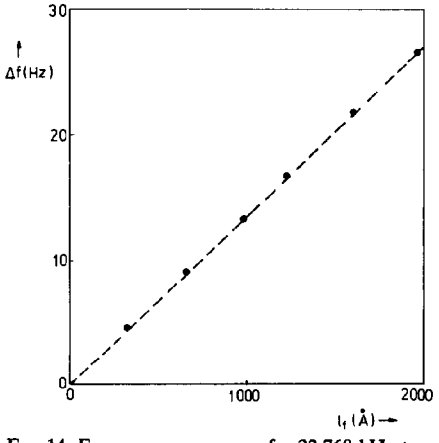

Fig 14 Frequency response of a 32 768 kHz tuning-fork-shaped quartz resonator coated by silver films

resonators vibrating in a thickness shear mode or in a compressional mode

The frequency response of a tuning-fork-shaped quartz resonator, widely used as a timer in wrist watches, was also checked Silver films were deposited on the small surfaces of the vibrating arms of the tuning fork The thickness of these depositions was measured by the adjacent sensing head of a quartz thickness monitor The experimental results are given in Fig 14, and show that the measured frequency shifts are proportional to the thickness of the silver films

From these experiments we can conclude that whatever the vibrational mode of the quartz resonators, their frequency decrease is related to the mass of the deposited film

5. Microweighing with resonators made of other piezoelectric materials

Quartz is the most widely used piezoelectric material for resonator manufacture It has several advantages when compared with other piezoelectric materials It is chemically inert, water insoluble and temperature resistant up to 573 °C, where α-quartz transforms into β-quartz Another advantage refers to the high quality factor of the quartz resonators, permitting an excellent frequency stability

One could further ask if the microweighing capability is exhibited only by quartz resonators To answer this question, some experiments were carried out to check the mass sensitivity of some resonators made of other piezoelectric materials

First a resonator made of PZT ceramic was tested It had a nominal frequency of 462 5 kHz One of its major faces was successively vacuum coated with copper films It was found that the mass of these films induced a frequency decrease of the PZT resonator The experimental results are shown in Fig 15, which reveals that the frequency decrease of the PZT resonator is proportional to the mass of the deposited film

Further a Z-cut resonator made of lithium niobate was tested The resonator had a diameter of 12 mm and a thickness of 3 84 mm Its nominal frequency was 922 kHz Such a resonator vibrates in a compressional mode [26], like the X-cut quartz resonators One of the major faces of the $LiNbO_3$ resonator was successively coated with copper films by vacuum deposition The experimental results are shown in Fig 16, which also reveals that the frequency decrease of the $LiNbO_3$ resonator is proportional to the mass of the deposited films As expected, the experimental points fit exactly the solid line drawn according to eqn (63) This result is very important, since $LiNbO_3$ might replace quartz in applications at higher temperatures The Curie point of $LiNbO_3$ is 1200 °C and it was found to be piezoelectrically useful up to 1050 °C [26]

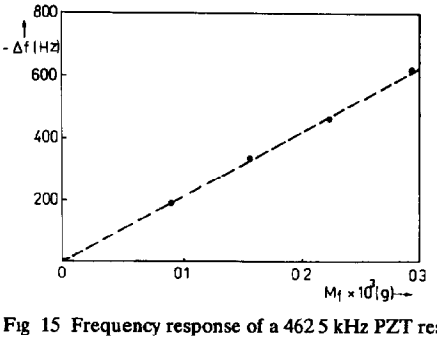

Fig 15 Frequency response of a 462 5 kHz PZT resonator coated by copper films

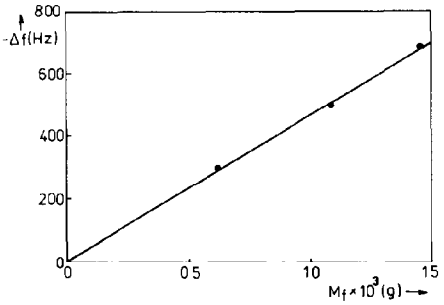

Fig 16 Frequency response of a 922 kHz $LiNbO_3$ resonator coated by copper films

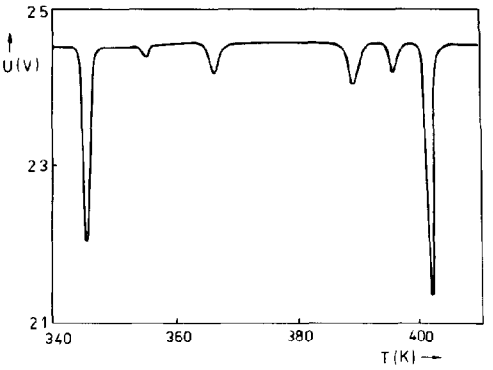

Fig 17 Vibrational amplitude change of a palladium-coated 5 MHz quartz-crystal resonator during a temperature sweep

6. Damping of the quartz resonator vibrations during a temperature sweep

Since Sauerbrey [1] introduced the quartz-crystal microbalance for thin-film mass measurements, most attention has been focused on the frequency change Meanwhile, this technique was extended by EerNisse [25] to thin-film stress measurements using the double-resonator technique and by van Ballegooijen [27] to temperature determination These two extensions used the vibrating frequency as the only measurable parameter Unfortunately, little attention was paid to the damping of the quartz-crystal vibrations King and Hoffman [28] recorded a quartz-crystal series-resistance variation during manganese deposition Scheide and Guilbault [29] recorded the cut-off frequencies of the coated quartz-crystal resonators, as the upper limit of the frequency shift before the complete damping of the quartz-crystal vibration Mecea and Bucur [20] showed, for the first time, that the damping of the quartz-crystal vibrations depends on the nature of the viscous layer deposited onto the quartz resonator surface This was also shown above in Section 2 6

A very interesting and reproducible phenomenon was observed when the rectified r f voltage U, as a measurable parameter of the quartz-resonator vibration amplitude, was recorded during a temperature sweep [30] A typical example is shown in Fig 17 The change in the vibration amplitude of a 5 MHz plane-parallel quartz-crystal resonator with 4500 Å thick, 7 mm diameter keyhole-shaped palladium electrodes was recorded during a temperature increase from 340 to 410 K, with a constant heating rate of 0 05 K s^{-1} We suppose that this phenomenon is due to dissipation of the vibration energy in the deposited film, at certain temperatures and frequencies, through a resonance phenomenon

In order to demonstrate that the deposited film, and not the quartz-crystal resonator, is responsible for the energy dissipation, the following experiment was performed

A 14 mm diameter, plane-parallel, 5 MHz, AT-cut quartz-crystal resonator was covered on both sides with keyhole-shaped 7 mm diameter palladium electrodes The palladium films were obtained by vacuum deposition at a rate of 20 Å s^{-1} Their thickness on each side was 3000 Å

The temperature sweep, in a purified argon flow, was performed in an electrically heated copper cell described elsewhere [31] This cell was also used for hydrogen sorption studies in thin palladium films [32, 33] The cell temperature was recorded on the X-axis of an X–Y recorder (Endim 620 02) using a chromel–alumel thermocouple The vibration amplitude of the quartz-crystal resonator was recorded as the rectified r f voltage U on the Y-axis

As the structure of the palladium films is strongly distorted by hydrogen absorption–desorption cycles [34], significant changes in the vibration-energy dissipation spectrum are expected If the quartz crystal alone is responsible for the vibration-energy dissipation spectrum, no changes in the spectrum are expected, because hydrogen is not absorbed in quartz

Hydrogen absorption–desorption cycles were performed with the arrangement currently used for sorption studies in thin palladium films [32, 33]

The palladium films, on both sides of the quartz resonator, were charged with hydrogen in the β-phase of the hydride, at atmospheric pressure and 354 K, until a steady frequency level was reached Then, the hydrogen flow was replaced by a purified argon flow and hydrogen desorption occurred After complete hydrogen desorption, the cell temperature was increased linearly from 290 to 430 K with a heating rate of 0 05 K s^{-1}, and the vibration-energy dissipation spectrum was recorded while purified argon was flowing over the coated quartz-crystal resonator Then the copper cell was allowed to cool down to room temperature, and the palladium films on the quartz-crystal resonator were investigated by X-ray diffraction

Several vibration-energy dissipation spectra are shown in Fig 18 They were obtained for as-deposited palladium films and for a different number of hydrogen absorption–desorption cycles Curve A was obtained for the freshly palladium-coated quartz-crystal resonator Curve B was obtained after three hydrogen absorption–desorption cycles Curve C was obtained after a total number of 10 hydrogen absorption–desorption cycles Curve D was obtained after a total number of 18 absorption–desorption cycles and curve E after 26 absorption–desorption cycles Further attempts to obtain such a spectrum after 34 absorption–desorption cycles were not successful because the quartz-crystal resonator was no longer vibrating, being completely damped

Each spectrum exhibits several vibration-energy dissipation peaks, also called deeps, in the recorded ΔU voltage Their magnitude changes continuously as the palladium electrodes are submitted to an increased number of hydrogen absorption–desorption cycles This is especially evident for the deeps at 369 K and those at 385 K

The X-ray diffraction measurements, as illustrated in Table 2, reveal a marked change in the palladium film structure after repeated hydrogen absorption–desorption cycles Where two measurements are recorded, they refer to the two palladium electrodes

The first three hydrogen absorption–desorption cycles induced the breaking of the crystallites and increased the mean-square deformation of the palladium lattice Further hydrogen absorption–desorption cycles induced an increase in the crystallite size and a new arrangement of the palladium lattice

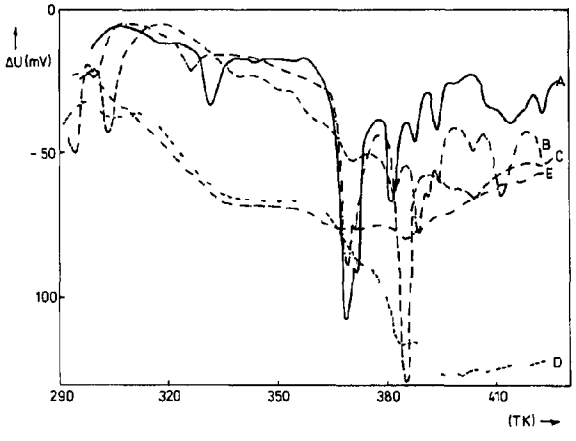

Fig 18 Vibration energy-dissipation spectra of a 3000 Å thick palladium film drawn for as-deposited palladium film and for a different number of hydrogen absorption–desorption cycles A, as deposited, B, 3 cycles, C, 10 cycles, D, 18 cycles, E, 26 cycles

TABLE 2 X-ray diffraction measurement results

Number of hydrogen sorption cycles	Mean-square deformation coefficient $\langle \epsilon^2 \rangle^{1/2}$	Mean crystallite size (Å)	Lattice parameter (Å)
0	0.775×10^{-5}	357	3 87
	0.921×10^{-5}	319	3 87
3	3.142×10^{-5}	163	3 92
18	2.678×10^{-5}	186	3 90
	2.658×10^{-5}	188	3 91
26	0.512×10^{-5}	560	3 85
	0.654×10^{-5}	450	3 85
34	0.370×10^{-5}	1156	3 86
	0.379×10^{-5}	952	3 86

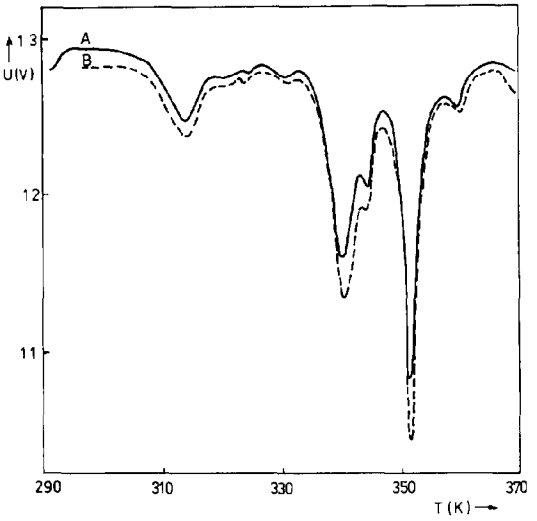

Fig 19 Vibration energy-dissipation spectra before (A) and after (B) a heat treatment of 2 h at 390 K

The change in the palladium electrode structure, while significant changes in the vibration-energy dissipation spectrum are recorded, is a valuable proof that a connection between the electrode structure and the vibration-energy dissipation spectrum should exist The exact correlation is not yet established Some additional experiments could help the understanding of this phenomenon

Figure 19 reveals changes that appeared in the vibration amplitude versus temperature spectrum of a quartz resonator with 2000 Å thick silver electrodes following a heat treatment in air Curve A indicates the vibrational-energy absorption spectrum for freshly deposited silver electrodes Curve B was drawn after a 2 h heat treatment at 390 K and cooling down to room temperature Both curves were recorded during the temperature increase Changes in the spectrum are

thought to be explained by changes in the deposited electrode structure

In another experiment the frequency of a quartz resonator was increased by inserting a series capacitor between the quartz resonator and the transistorized oscillator circuit, thus diminishing the equivalent series capacitance of the resonant circuit Figure 20 shows the translation to lower temperatures of the voltage deeps corresponding to resonant energy absorption, while increasing the frequency of the coated quartz resonator These frequencies, at room temperature, are indicated on each curve Curve A was drawn without a series capacitor Curve B was drawn after the insertion of a 47 pF capacitor and curve C was drawn after the insertion of a 22 pF capacitor This experiment proves that the temperature and frequency of the resonant energy absorption are correlated

Figure 21 reveals the effect of the electrode-surface etching on the vibrational-energy absorption spectrum A 5 MHz quartz resonator, with 600 Å thick silver electrodes, was successively etched in an argon plasma Curve A was drawn before plasma etching Curve B was drawn following plasma etching of 77 Å silver from

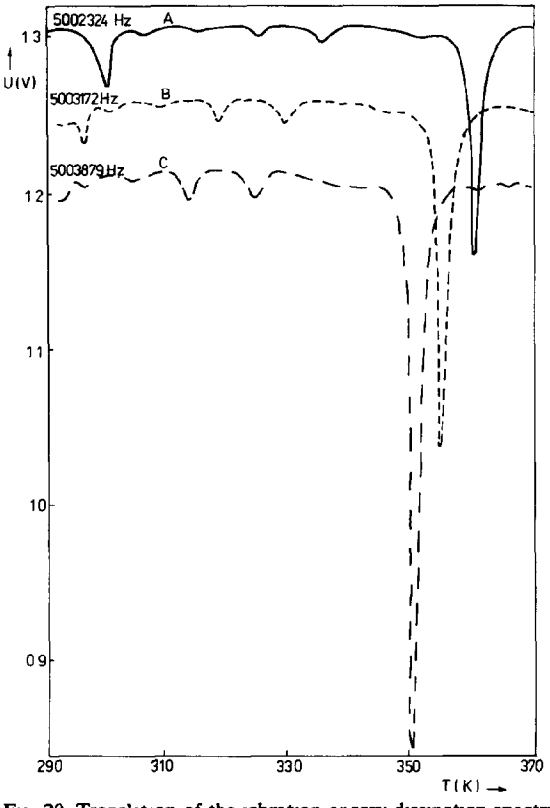

Fig 20 Translation of the vibration energy-dissipation spectrum of a quartz-crystal resonator coated with 2000 Å silver-film electrodes following the change of its vibrational frequency by the insertion of a series capacitor

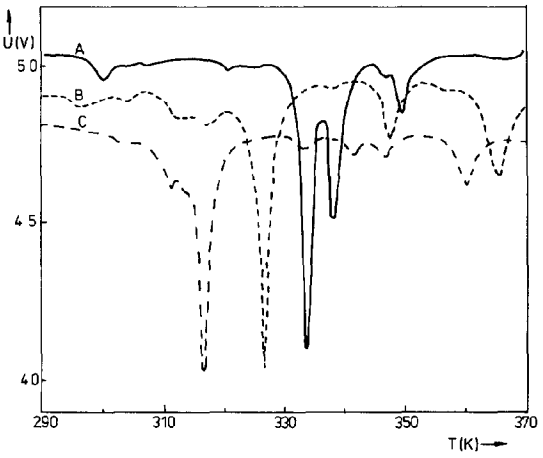

Fig 21 Vibration energy-dissipation spectra of a quartz-crystal resonator coated with 600 Å silver electrodes following successive electrode argon plasma etching A, as deposited, B, 77 Å silver etched from one electrode, C, 115 Å silver etched from the other electrode

one of the electrodes Curve C was drawn after etching of 115 Å silver from the other electrode This experiment proves that the vibrational-energy absorption spectra are very sensitive to treatment of the thin-film surface

A very interesting conclusion, derived from the energy transfer model, is that whenever the compound resonator vibration amplitude diminishes, an increase of the compound resonator frequency is expected Thus we have

$$\frac{\partial \omega_c}{\partial A_{1q}} = -2\frac{\rho_q l_q \omega_q^2}{\rho_f v_f}\frac{A_0^2}{A_{1q}^3}\left\{1-\exp\left[-2\left(\frac{\omega_c}{2\nu_f}\right)^{1/2} l_f\right] + \frac{\omega_c l_f}{(2\nu_f \omega_c)^{1/2}}\exp\left[-2\left(\frac{\omega_c}{2\nu_f}\right)^{1/2} l_f\right]\right\} < 0$$

This derivative is always negative, leading to the mentioned correlation between the vibration amplitude and frequency of the compound resonator This is proved experimentally in Fig 22, where both frequency and amplitude versus temperature characteristics of an AT-cut quartz resonator are drawn It is evident that to each recorded voltage deep corresponds an increase of the quartz resonator frequency This observation is very important When using a quartz-crystal resonator as a frequency standard, it is compulsory to be out of a resonant energy absorption to get a better frequency stability

7. Applications of the vibrating quartz sensors

A common feature of all the theoretical developments previously presented is that they were stimulated by the large range of possible applications of vibrating

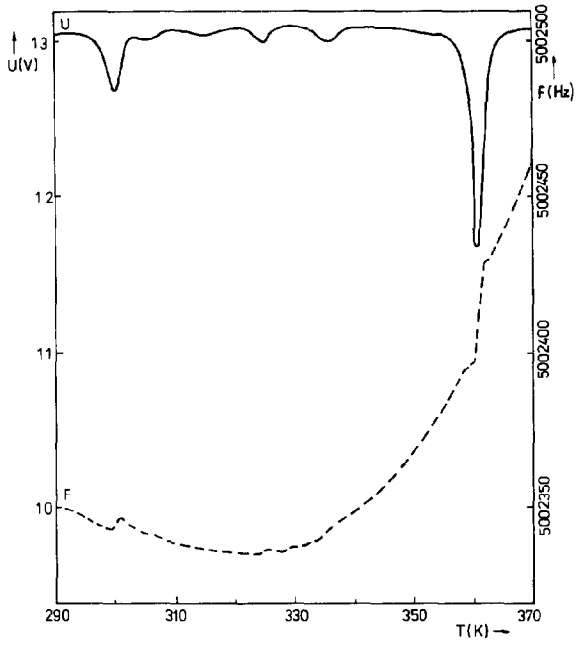

Fig 22 Simultaneous record of vibration energy-dissipation spectrum and frequency vs temperature characteristics of an AT-cut quartz-crystal resonator coated with 2000 Å silver electrodes

quartz sensors It is very difficult to present here all the possible applications, which cover the following fields

(i) thin-film thickness monitoring in physical vapour deposition,

(ii) gas sorption by different coatings of the quartz resonators,

(iii) mass measurements and viscous effects in liquids

An excellent monograph on quartz-crystal microbalance applications was edited by Lu and Czanderna [11, 14, 25] This Section presents other applications that we have developed over the years

7 1 Sorption measurements with vibrating quartz sensors

When a surface is exposed to an ambient different from that with which it has reached equilibrium, mass changes may occur due to sorption (absorption or desorption) This may be physisorption or chemisorption, each type having its own characteristics The very high sensitivity of quartz resonators to mass changes, 1×10^{-12} g cm^{-2} as reported by Warner and Stockbridge [35], is very profitable for sorption studies Unfortunately, when changing the ambient of a shear vibrating quartz-crystal resonator, both the frequency and vibration amplitude may change The relative change of these parameters will be a superposition of the various influences acting on them Thus, we have

$$\frac{\Delta f}{f}=\left(\frac{\Delta f}{f}\right)_M+\left(\frac{\Delta f}{f}\right)_T+\left(\frac{\Delta f}{f}\right)_S+\left(\frac{\Delta f}{f}\right)_p+\left(\frac{\Delta f}{f}\right)_\eta+\left(\frac{\Delta f}{f}\right)_A \tag{64}$$

$$\frac{\Delta U}{U}=\left(\frac{\Delta U}{U}\right)_\nu+\left(\frac{\Delta U}{U}\right)_R$$

where $(\Delta f/f)_M$ represents the pure mass effect on the resonance frequency of the quartz resonator With sorption studies the mass of the adsorbed gas is rather small, so that eqn (3), initially derived by Sauerbrey, might be used

$$\left(\frac{\Delta f}{f}\right)_M=-\frac{m_g}{m_q}$$

where m_g is the mass of the gas absorbed by the unit of surface of the coating

$(\Delta f/f)_T$ is the partial effect of the temperature on the total relative frequency change This becomes important when the sorption is either endothermal or exothermal Otherwise, sorption measurements are always performed at a constant temperature, its contribution being neglected

$(\Delta f/f)_S$ is the partial effect of the stress on the total relative frequency change This effect was revealed by EerNisse [25] and becomes important when changes of the lattice parameter are induced by gas absorption, as in the case of hydrogen (deuterium) absorption by thin palladium films, as revealed by Bucur and Flanagan [36] This unwanted effect can be circumvented either by the use of the double-resonator technique, as proposed by EerNisse [25], or by the use of quartz resonators having an SC-cut (stress-compensated cut) [25]

$(\Delta f/f)_p$ is the partial effect of the hydrostatic pressure on the total relative frequency change The magnitude of this effect was evaluated by Warner [37] We have $(\Delta f/f)_p=+13\,5\times10^{-10}$ Torr^{-1} for AT-cut quartz resonators at 323 K with a nearly linear variation with temperature of $-0\,015\times10^{-10}$/K

$(\Delta f/f)_\eta$ is the partial effect of the shear impedance of the gas on the total relative frequency change [37] Its magnitude is expressed by

$$\left(\frac{\Delta f}{f}\right)_\eta=0\,72\times10^{-6}(\pi f_c\rho_g\eta_g)^{1/2}$$

Here ρ_g and η_g are the density and viscosity of the gas, respectively

$(\Delta f/f)_A$ is the partial effect of a change in the vibrational amplitude of the quartz resonator following the gas sorption This was revealed in Section 6

$(\Delta U/U)_\nu$ is the partial effect of the gas kinematic viscosity on the vibration amplitude of the quartz resonator This is particularly important when a phase transition occurs in the deposited film

$(\Delta U/U)_R$ is the partial effect of a resonance phenomenon occurring in the vibrating film

Although many factors affect both the measured parameters, frequency and vibration amplitude, of a coated quartz resonator, this is not a dramatic situation The partial effects are either negligible or can be eliminated by using a differential method for measurements This implies the use of two identical quartz resonators, one of them being coated with the active film and the other being coated with a neutral film Thus, the temperature, hydrostatic pressure and shear impedance of the gas will have no significant effect on the accuracy of the sorption measurements For the case of absorption measurements, accompanied by lattice parameter changes, the use of two quartz resonators with SC-cut, in a differential system, is the best solution Temperature control of the measuring cell is compulsory, because the sorption equilibrium is strongly affected by the temperature

7 2 Hydrogen (deuterium) sorption in thin palladium films

Quartz-crystal resonators proved to be very useful for hydrogen (deuterium) sorption studies in thin palladium films The very high mass sensitivity and fast response of these sensors were the attractive features recommending them for such studies

It is well known [34] that palladium selectively and reversibly absorbs large amounts of hydrogen, or its isotopes, when its clean and active surface comes in contact with these gases Although hydrogen is the lightest chemical element, the uptake of this gas can be followed using palladium films deposited onto the electrode surface of the quartz resonators, or using palladium as the electrode material The very fast time response of these quartz mass sensors is also useful for kinetic measurements

Some characteristic absorption–desorption curves are shown in Fig 23 Its reveals that equilibrium is rapidly attained with both hydrogen and deuterium The equilibrium is indicated by the constancy of the frequency shift during absorption and by the constant level attained after every hydrogen (deuterium) desorption cycle with nitrogen gas For these measurements an AT-cut quartz-crystal resonator with a nominal frequency of 8 35 MHz

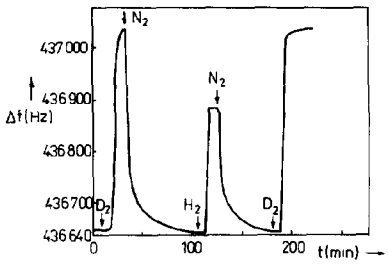

Fig 23 The absorption–desorption curves for hydrogen and deuterium (β-phase)

was used The numerical results are shown in Table 3 Here ΔF_{Pd} represents the frequency decrease following the electrochemical deposition of Pd films onto both gold electrodes of the quartz resonator, ΔF_H and ΔF_D represent the measured frequency decreases following hydrogen and deuterium absorption, respectively, ΔF_H^{calc} and ΔF_D^{calc} represent the expected frequency decrease following hydrogen and deuterium absorption, taking the hydrogen (deuterium) to palladium atomic ratio to be 0 68 [34] for absorption in the β-phase at atmospheric pressure, H/Pd and D/Pd represent the measured isotope to palladium ratios, H/D is the measured ratio of the two isotopes in palladium at equilibrium and T is the temperature of the experiment

The results shown in Table 3 reveal that hydrogen and deuterium absorption in palladium induce a larger frequency shift than expected taking into account the hydrogen to metal ratio of 0 68 for the β-phase of the hydride reported in the literature [34] We got H/Pd and D/Pd ratios larger than 0 68 This might be explained by the additional frequency decrease induced by the mechanical stresses developed in the quartz by the increase of the lattice parameter of palladium, following hydrogen and deuterium absorption

Hydrogen sorption studies can be performed not only in the β-phase (saturated) of the hydride, but also in the α-phase, at low hydrogen partial pressure [32] This pressure can be obtained by mixing a controlled hydrogen flow with a controlled flow of an inert gas (helium, argon or nitrogen) The partial pressure ranges used were 0 27–9 45 kPa for hydrogen and 0 3–16 4 kPa for deuterium at a constant temperature of 353 K. Purified nitrogen at a constant flow was used as an inert gas, both for mixing with hydrogen or deuterium and for desorption Its flow rate was 50 ml/min The chemical stability of the nitrogen in the presence of hydrogen and palladium was checked by substituting helium for nitrogen There was no difference in the observed desorption rates

The working mass sensor was an AT-cut quartz-crystal resonator, having a nominal frequency of 5 27 MHz, which was covered on both sides with palladium layers by electrodeposition onto the silver electrodes

TABLE 3 Numerical data on hydrogen and deuterium measurements in thin palladium films

f_q (MHz)	ΔF_{Pd} (Hz)	ΔF_H (Hz)	ΔF_H^{calc} (Hz)	ΔF_D (Hz)	ΔF_D^{calc} (Hz)	H/Pd	D/Pd	H/D	T (K)
	63204	655	407	990	800	1 10	0 83	1 32	299
8 35	61766	548	399	817	787	0 94	0 70	1 34	300 3
	55078	814	356	1082	700	1 57	1 04	1.50	300

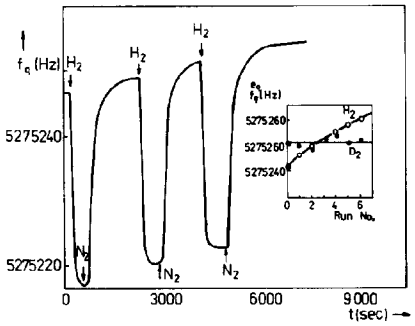

Fig 24 The absorption–desorption curves for hydrogen in the α-phase of the palladium hydride Inset the effect of remanent elastic stresses on the desorption steady-state frequency values for hydrogen (O) and deuterium (●)

The experimental results for three successive hydrogen sorption cycles at a constant pressure of 9 45 kPa are shown in Fig 24 Because of the introduction of a certain small flow of hydrogen (indicated by H_2 arrows) in the flowing nitrogen gas, the frequency decreases to a steady-state value, which is ascribed to the equilibrium of the palladium layer with the gaseous hydrogen At the time indicated by N_2 arrows, pure nitrogen was allowed to flow through the cell, thus removing the absorbed hydrogen The equilibrium frequency was higher than the previous one This shift of the desorption steady-state frequency value (f_q^{eq} in the inset of Fig 24) is ascribed to the irreversible changes in the structure of the palladium layer during the uptake of hydrogen. No such effect was found for deuterium Deuterium induces smaller elastic stresses and does not affect the structure of the palladium layer, the F_q^{eq} values remain constant during the sorption cycles, as revealed by the inset of Fig 24

These experiments proved the additional effect of the elastic stresses on the vibrational frequency of an AT-cut quartz resonator This unwanted effect can be eliminated, as already mentioned, by the use of a stress-compensated cut, called the SC-cut

7 3 Moisture sorption in a hygroscopic polymer

When a quartz-crystal resonator is coated with a hygroscopic material it becomes a very sensitive moisture sensor Du Pont Company was the first to use these

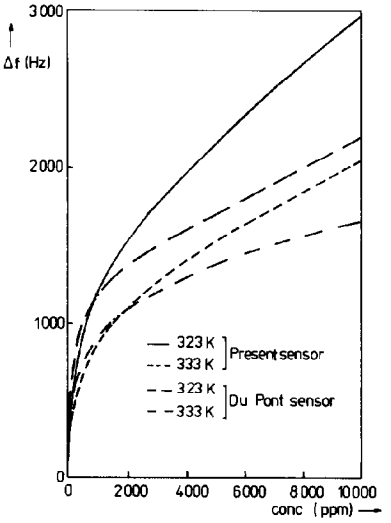

Fig 25 Frequency response to moisture of two different quartz-resonator moisture sensors

sensors down to a concentration of 0 1 ppm moisture in a permanent non-corrosive gas

Due to their polar nature, water molecules are strongly adsorbed by practically all solid surfaces at normal temperatures and pressures This is, in fact, the main problem in measuring accurately the moisture content of the permanent gases Reliable measurements can hardly be performed when this aspect is ignored A reliable calibration of all moisture sensors, mainly in the low concentration range, requires some experience However, this is possible in different ways that are described in the literature We chose a very simple and reliable method to calibrate the quartz-resonator moisture sensors A vacuum deposition plant was used for this purpose Following a careful evacuation of the bell jar, controlled amounts of water were injected with a microsyringe through a silicone rubber septum A quartz-crystal resonator coated on both sides with a natural polymer was accommodated in a temperature-controlled copper cell, where tween cavities were hollowed In one of these cavities was located the polymer-coated quartz resonator, while an identical uncoated quartz resonator was located in the other cavity This differential arrangement was used to measure the response of a quartz-resonator moisture sensor to various

concentrations of water The results obtained at 323 and 333 K are shown in Fig 25 The nominal frequency of the quartz resonators was 10 MHz The response of a Du Pont moisture sensor is also shown for comparison It is very clear that both sensors are very sensitive, mainly for moisture concentrations lower than 500 ppm Their sensitivities are temperature dependent, because the equilibrium between the gas phase and absorbed state is greatly affected by the absorbent temperature Figure 25 also reveals that the sensitivity of the present sensor, at the same temperature, is higher than that of the Du Pont moisture sensor

8. Tunable gas sensors

One of the main ideas of the energy transfer model is that whenever a medium is in contact with the vibrating surface of a quartz resonator, they together form a compound resonator whose frequency and vibration amplitude are greatly affected by the characteristics of the medium vibrating synchronously with the quartz resonator surface

The interaction of a shear vibrating quartz resonator with solid and liquid substances has already been described It is well known that shear waves do not propagate in gases However, if compressional waves are generated by an X-cut quartz resonator, ultrasonic longitudinal waves will propagate in the surrounding gas If the surrounding gas is induced to resonate at the same frequency as that of the quartz resonator, then an important amount of the vibration energy of the quartz resonator will be absorbed by the resonating gas The resonance condition can easily be accomplished when standing waves are generated between the surface of the quartz resonator and the surface of a parallel reflecting wall Standing waves are generated whenever the distance l between the two parallel surfaces is an integer number of halfwavelengths of the ultrasound generated by the quartz resonator

$$l = n\frac{\lambda}{2} = n\frac{v_g}{2f_q} \tag{65}$$

where v_g is the ultrasound velocity in the gas filling the resonance cavity and f_q is the frequency of the quartz resonator vibrating in a compressional mode

There can be a significant amount of vibration energy absorbed by the resonating gas, inducing the complete damping of the quartz-resonator vibrations

There seems to be a close analogy between the absorption of vibration energy by a gas at resonance in contact with a quartz resonator vibrating in a compressional mode and the absorption of vibration energy, at certain temperatures, by a solid film coating the surface of a shear vibrating quartz resonator

The gas-resonance condition, indicated by eqn (65), reveals that, for the same quartz resonator vibrating in a compressional mode, the resonance depends on the nature of the gas through the ultrasound velocity For some common gases the ultrasound velocities at 0 °C are given in Table 4 [38]

There is a significant difference in ultrasound velocity between various gases This feature can be used for gas detection Whenever the distance l between the surface of the quartz resonator and the surface of the reflecting wall is adjusted to fulfil the resonance condition for a certain reference gas, the presence of a small amount of another gas, differing in ultrasound velocity, will after the resonance and a change in the vibration amplitude of the quartz resonator will be recorded This is shown in Fig 26 for the case of a resonant cavity adjusted so that the distance between the surface of a 1 MHz quartz resonator and the surface of the reflecting wall is l_0 when air flows between the two surfaces The recorded signal related to the vibration amplitude of the quartz resonator is U_1, smaller than the maximum signal U_0 corresponding to the out-of-resonance condition When the air flowing through this cavity contains a small amount of hydrogen, the ultrasound velocity in such a mixture is higher than in

TABLE 4 Ultrasound velocities in some common gases at 0 °C

Gas	v_g (m/s)
Hydrogen	1269 5
Helium	972
Methane	472
Carbon monoxide	337 1
Nitrogen	337
Air	331 36
Nitric oxide	325
Oxygen	317 2
Argon	307
Nitrous oxide	261 8
Carbon dioxide	258
Sulphur dioxide	216 2
Carbon disulfide	189

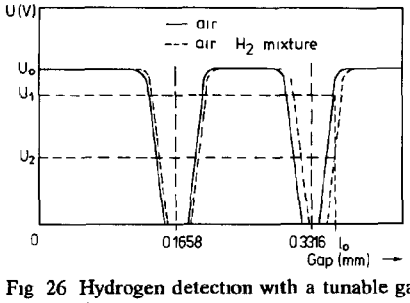

Fig 26 Hydrogen detection with a tunable gas sensor Example is given for $n=2$

pure air and a significant change in the recorded signal will be detected, the resulting voltage being U_2

The gap between the quartz-resonator surface and the reflecting-wall surface can be adjusted to be close to the resonance condition for whatever gas Thus, we can call such a sensor 'tunable gas sensor' Whenever a gas differing in ultrasound velocity is temporarily present in the gas for which the cavity was tuned, a measurable change in the rectified r f voltage, corresponding to the new vibration amplitude, will be recorded

This detection principle was first patented by Mecea and Bucur [39] and was used by Mecea and Tatar for hydrogen detection in air [40]

The resonance condition (65) is affected by temperature changes through the cavity dilatation, according to the law

$$l = l_0(1 + \alpha t) \tag{66}$$

and through the ultrasound velocity change according to the law

$$v = v_0(1 + t/273\ 15)^{1/2} \tag{67}$$

These two major effects can alter the reliability of a tunable gas sensor Good temperature control of the detection cell is very important However, the adverse effect of the temperature changes can be greatly diminished by thermocompensation This is accomplished when the dilatation of the gap l_0 follows the change of the resonance condition (65) through the temperature dependence of the ultrasound velocity In order to match the dilatation of the gap to the change of the ultrasound velocity, a detection cell was designed and is schematically shown in Fig 27 The quartz resonator, with a nominal frequency of 1 MHz and a diameter of 20 mm, is accommodated within the body of the cell To avoid mechanical losses, the quartz resonator is fixed in its nodal vibrational plane The electrical connections to the evaporated Au/Cr electrodes touch the quartz resonator in its nodal vibrational plane too

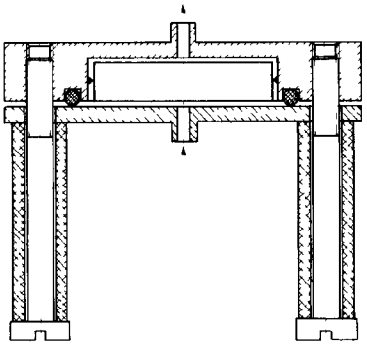

Fig 27 Schematic drawing of a thermocompensated tunable gas sensor

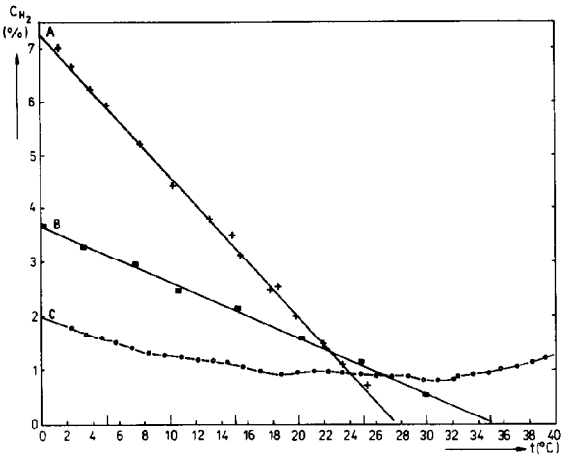

Fig 28 Effect of the thermocompensation on a tunable gas sensor, when hydrogen is detected in air A, without thermocompensation, B, unsatisfactory thermocompensation For B and C different lengths of ceramic cylinders were used

The gas enters the cell through a pipe penetrating the lid and exits through a pipe emerging from the body of the cell A rubber gasket hermetically closes the cell It also allows the lid to move following the dilatation of the aluminum screws, which rest on the lid surface by means of ceramic cylinders with a very small dilatation Their length is calculated to match the dilatation of the gap to the ultrasound velocity change due to a temperature change As eqn (67) is not linear like the dilatation law, the best thermocompensation is obtained in a rather narrow temperature range, as shown in Fig 28 for for the case of hydrogen detection [41]

8 1 Hydrogen detection

In recent years hydrogen has become one of the most useful gases Many industries, such as chemical, metallurgical and food, use hydrogen as a raw material

The increasing use of hydrogen gas should not be considered as being without disadvantages A hydrogen leak in the atmosphere should be avoided, because hydrogen, when mixed with air in the ratio 4 00–74 2 vol %, is explosive [42] For this reason, among others, it has become very important to develop highly sensitive hydrogen sensors to prevent accidents due to hydrogen gas leakage, thus saving lives and equipment Such sensors should allow continuous monitoring of the concentration of gases in the environment in a quantitative and selective way

Several classes of hydrogen detectors have been developed semiconductor, pyroelectric, piezoelectric and electrochemical devices The common feature of all these sensors is that they use a catalyst, mainly palladium, to detect hydrogen selectively The main drawback of these sensors is the possibility of catalyst

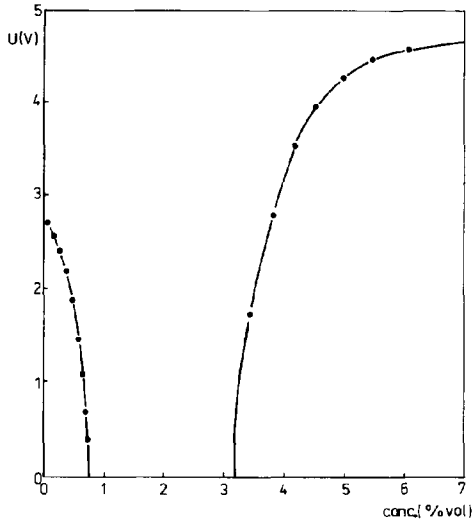

Fig 29 Response of the tunable gas sensor to various concentrations of hydrogen in air at 310 K

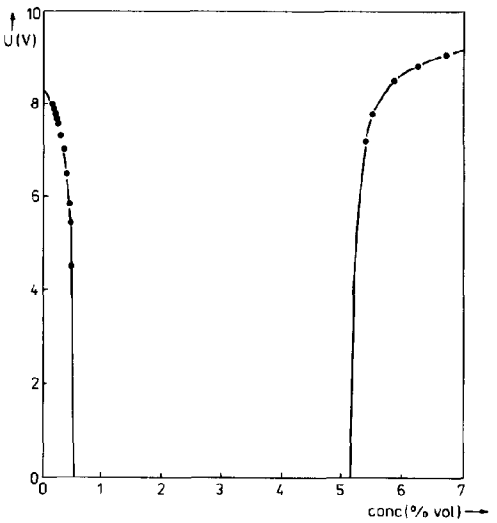

Fig 30 Response of the tunable gas sensor to various concentrations of hydrogen in argon

poisoning by sulphur dioxide, hydrogen sulfide, carbon monoxide, sulphur and other gases Consequently they can work properly only in controlled atmospheres

It has already been proved that the working principle of a tunable gas sensor can be used for hydrogen detection in air [40, 41] Here new experimental results are shown By tuning the gap l_0 to get the near-resonance condition for air, it was possible to record the response of the sensor to various concentrations of hydrogen in air The results are shown in Fig 29, where the resonance deep is revealed in a rather large hydrogen concentration range, 0 75–3 1 vol % hydrogen in air This is because of the strong vibration-energy absorption by the resonating gas A similar result was obtained for hydrogen–argon mixtures when the gap l_0 was tuned to get the near-resonance condition for argon The sensor response for different concentrations of hydrogen in argon is shown in Fig 30 Here the resonance deep is broader than in the case of air because of the higher molecular weight and viscosity of the argon gas

The time response of such a sensor is very fast, depending on the necessary time to fill the detection cavity with the new concentration of the gas This is revealed in Fig 31 for various concentrations of hydrogen in air Measurements were performed at 310 K

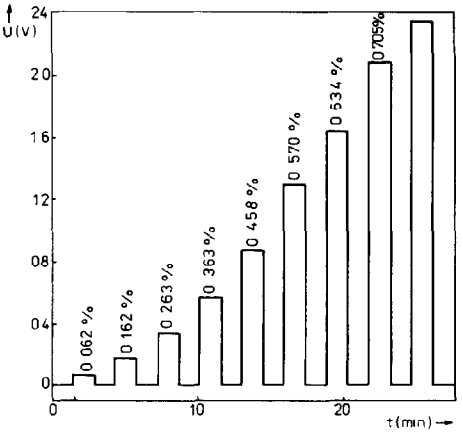

Fig 31 Time response of the tunable gas sensor for various concentrations of hydrogen in air at 310 K

8 2 Methane detection

Interest in methane detection arises from its wide domestic use When mixed with air in the ratio 5 00–15 00 vol % it is also explosive [42] As shown in Table 4, the ultrasound velocity in methane is different from that in the air, allowing its detection with a tunable gas sensor As expected, the sensitivity of a tunable gas sensor for methane detection in air will be smaller than that for hydrogen detection because the ultrasound velocity in methane is closer to that in air than in the case of hydrogen This is shown in Fig 32, where the response of the tunable gas sensor for various concentrations of hydrogen and methane in air at 310 K is revealed The result shown in Fig 31 proves that the sensitivity of the tunable gas sensor for each of these gases is very high, allowing their detection in the environment at concentrations much lower than the explosion limits This is a very promising application of tunable gas sensors

8 3 Gas-chromatography detector

A tunable gas sensor might also be used as a universal gas-chromatography detector The detection of various

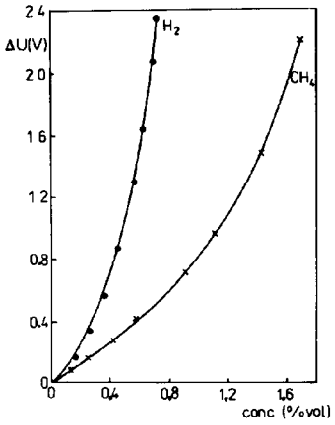

Fig 32 Response of a tunable gas sensor to various concentrations of hydrogen and methane in air at 310 K

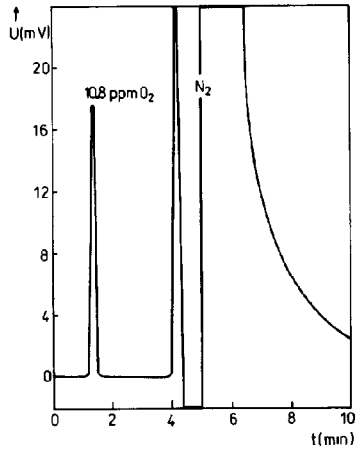

Fig 33 Response of a tunable gas sensor when used as a gas-chromatography detector at 310 K

gases is based on the existing difference in ultrasound velocities

In order to check the performance of a tunable gas sensor as a detector for gas-chromatography, the gap between the quartz-resonator surface and the reflecting wall was tuned to the near-resonance condition for hydrogen, which was the eluent gas of a gas-chromatograph A gas sample containing 10 8 ppm oxygen in a nitrogen matrix was used (can mix No 48 from Scott Analyzed Gases) As shown in Fig 33, the separated oxygen peak is sensitively detected by a tunable gas sensor The nitrogen peak is very large and discontinuous This is because of the very large concentration of nitrogen, which caused the whole resonance deep to be swept, including the situation of complete damping of the quartz-resonator vibrations

When using a conventional thermal-conductivity detector the oxygen was not detected and the nitrogen peak was much narrower This proves the very high sensitivity of a tunable gas sensor when used as a gas-chromatography detector

9. 'Nanobalance' experiment in outer space

One of the chief virtues of quartz resonators is that they can work in both vacuum conditions and controlled atmospheres

The very high sensitivity of the shear vibrating quartz resonators to the mass of a deposited film was proved to be profitable for studies on the stability of thin layers of silicone dioxide in outer space It was thought that cosmic radiation and high-energy particle bombardment could sputter such a layer, which could be useful for the protection of the optical equipment of satellites and space laboratories

In order to check the behaviour of a silicone dioxide protective layer in a severe cosmic environment, two AT-cut quartz-crystal resonators with a nominal frequency of 6 2 MHz were coated by vacuum deposition with 6000 Å layers of silicone dioxide on one side One of these resonators could be exposed to the cosmic environment by actuating an electromagnetic shutter, while the other, situated in the close neighbourhood, could not The difference between the two frequencies was converted into an analog signal and, through the telemetry system, recorded on the Earth

This experiment called 'Nanobalance' was performed during the Soviet–Romanian joint space flight on the space laboratory 'Salut-6' (14–21 May, 1981)

The measuring device was located in an experimental enclosure near the wall of the space laboratory It was exposed to the cosmic environment by opening the external lid of the experimental enclosure

The experimental results are shown in Fig 34 The steady signal, recorded for a day and a half, revealed a good stability of the silicone dioxide layer in the cosmic environment Before the end of the day of 18 May, an increase in the mass of the silicone dioxide layer was recorded This continued up to the limit of the telemetry range The solar explosion on 16 May

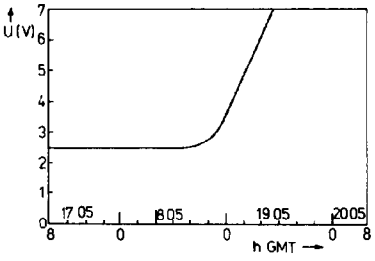

Fig 34 Record of the 'Nanobalance' signal when exposed to the cosmic environment

(8 07–8 34 GMT) was responsible for this effect The start of this deposition was delayed by 59 5 h from the solar explosion, resulting in a speed of 697 7 km/h for the solar wind This wind drove cosmic dust towards the Earth and a thin layer of cosmic dust was deposited onto the surface of the quartz resonator when the shutter was opened

After flight, measurements revealed that $8\,62\times10^{-6}$ g of cosmic dust was deposited Auger electron spectroscopic analysis of this deposition revealed silicone and oxygen atoms from the silicone dioxide layer, carbon, nitrogen, sulphur and hydrogen, probably from an organic contamination, and aluminium, titanium and iron atoms from the cosmic dust

This experiment proved the excellent behaviour of a quartz-resonator mass sensor in the cosmic environment It also proved the good stability of silicone dioxide protective layers in the severe cosmic environment and the effect of solar explosions regarding the deposition of cosmic dust layers onto the surfaces of satellites and space laboratories

10. Conclusions

The theoretical and experimental contributions revealed in this paper lead to the following conclusions

(1) Whenever a coating (solid film, liquid layer or gas at resonance) is in contact with the antinodal surface of a quartz resonator, the vibrational characteristics of the compound resonator thus formed, namely the nominal frequency and vibration amplitude, are correlated to the physical characteristics of the coating

(2) The energy transfer model describes the interaction of whatever coating, either solid or liquid, with the vibrating quartz substrate It also explains the correlation between the mass-sensitivity distribution and vibration-amplitude distribution on the surface of the quartz resonators

(3) The microweighing capability is not restricted to shear vibrating quartz resonators (AT or BT cuts), but extends to any quartz-crystal cut and vibrational mode, providing that the coating covers the antinodal surfaces of these resonators

(4) The microweighing capability is not restricted to quartz resonators, but extends to any piezoelectric resonator, when coated on its antinodal surfaces

(5) Damping of a coated quartz-resonator vibrations, at certain temperatures and frequencies during a temperature sweep, is correlated to the deposited film morphology and might develop as thin-film vibration spectroscopy

(6) Damping of the vibrations of a quartz resonator, vibrating in a compressional mode, when it is in contact with a gas at resonance, leads to a new sensing principle and the development of tunable gas sensors

(7) Vibrating quartz is not a simple weighing device, but rather a complex sensor that reveals many characteristics of a coating when both the nominal frequency and vibrational-amplitude changes are monitored It is not a single instrument, but rather an orchestra, playing the wonderful symphony of the surface and interfacial phenomena

Acknowledgements

The author would like to thank to his mentor, R V Bucur of the Department of Inorganic Chemistry, Uppsala University, Sweden, for 17 years of work together, sharing exciting results and disappointments His continuous support, suggestions and encouragements are gratefully acknowledged

References

1 G Sauerbrey, Use of vibrating quartz for thin film weighing and microweighing (in German), *Z Phys*, *155* (1959) 260–222
2 G Sauerbrey, Measurement of very small vibration amplitude of vibrating plates by light beam modulation (in German), *Z Phys*, *178* (1964) 457–471
3 G Sauerbrey, Effect of the electrode dimensions on the vibration area of thin quartz plates (in German), *Arch Electron Ubertragungstech*, *18* (1964) 617–622
4 H K. Pulker, Research on continuous thickness measurement on thin evaporated films with a vibrating quartz device (in German), *Z Angew Phys*, *20* (1966) 537–540
5 R M Mueller and W White, Direct gravimetric calibration of a quartz crystal microbalance, *Rev Sci Instrum*, *39* (1968) 291–295
6 C D Stockbridge in K H Behrndt (ed), *Vacuum Microbalance Technique*, Vol 5, Plenum, New York, 1966, p 193
7 F Boersma and E C van Ballegooijen, Rotated *Y*-cut quartz crystal with two different electrodes treated as a one-dimensional acoustic composite resonator, *J Acoust Soc Am*, *62* (1977) 335–340
8 J G Miller and D I Bolef, Acoustic wave analysis of the operation of quartz crystal film-thickness monitors, *J Appl Phys*, *39* (1968) 5815–5816
9 K.H Behrndt, Long term operation of crystal oscillators in thin film deposition, *J Vac Sci Technol*, *8* (1971) 622–626
10 C S Lu and O Lewis, Investigation of film-thickness determination by oscillating quartz resonators with large mass load, *J Appl Phys*, *43* (1972) 4385–4390
11 C Lu in C Lu and A W Czanderna (ed), *Application of Piezoelectric Quartz Crystal Microbalances*, Elsevier, Amsterdam, 1984, p 41
12 E Benes, Improved quartz crystal microbalance technique, *J Appl Phys*, *56* (1984) 608–626
13 P L Konash and G J Bastiaans, Piezoelectric crystals as detectors for liquid chromatography, *Anal Chem*, *52* (1980) 1929–1931
14 A P M Glassford in C Lu and A W Czanderna (eds), *Applications of Piezoelectric Quartz Crystal Microbalances*, Elsevier, Amsterdam, 1984, pp 281–350

15 K K. Kanazawa and J G Gordon II, The oscillation frequency of a quartz resonator in contact with a liquid, *Anal Chim Acta, 175* (1985) 99–105
16 K K. Kanazawa and J G Gordon II, Frequency of a quartz crystal microbalance in contact with a liquid, *Anal Chem, 57* (1985) 1770–1771
17 V Mecea and R V Bucur, The mechanism of the interaction of thin films with resonating quartz crystal substrates the Energy Transfer Model, *Thin Solid Films, 60* (1979) 73–84
18 R P Feynman, R B Leighton and M Sands, *The Feynman Lectures on Physics,* Adison–Wesley, Reading, MA, 1966, p 24-1
19 L E Landau and E M Lifschitz, *Mecanique des Fluides,* Mir, Moscow, 1971, p 111
20 V Mecea and R V Bucur, The use of RF-voltage in quartz crystal microbalance measurements application to nonmetallic films, *J Phys E Sci Instrum, 7* (1974) 348–349
21 H K. Pulker, E Benes, D Hammer and E Solner, Progress in monitoring thin film thickness with quartz crystal resonators, *Thin Solid Films, 32* (1976 27–33
22 V M Mecea, A new method of measuring the mass sensitive area of quartz crystal resonators, *J Phys E Sci Instrum,* (1989) 59–61
23 L Wimmer, S Hertl, J Hemetsberger and E Benes, New method of measuring vibration amplitudes of quartz crystals, *Rev Sci. Instrum, 55* (1984) 605–609
24 G Horvath and L Aranyi, Alternative theoretical derivation of response function for coated shear-mode quartz piezoelectric crystals, *Analyst, 112* (1987) 1451–1452
25 E P EerNisse in C Lu and A W Czanderna (eds), *Applications of Piezoelectric Quartz Crystal Microbalances,* Elsevier, Amsterdam, 1984, pp 125–149
26 O E Mattiat (ed), *Ultrasonic Transducer Materials,* Plenum, New York, London, 1971, pp 148–151
27 E C van Ballegooijen, Simultaneous mass and temperature determination using a single quartz wafer an optimized crystal cut, *J Appl Phys, 50* (1979) 91–101
28 D King and G R Hoffman, Observation on a quartz deposition monitor, *J Phys E Sci Instrum., 4* (1971) 993–999
29 E P Scheide and G G Guilbault, Piezoelectric detectors for organophosphorus compounds and pesticides, *Anal Chem, 44* (1972) 1764–1768
30 V M Mecea, R V Bucur and E Indrea, On the possibility of thin film structure study with a quartz crystal microbalance, *Thin Solid films, 171* (1989) 367–375
31 V Mecea and R V Bucur, Piezoelectric quartz crystal microbalance (PQCMB) for sorption studies under dynamic conditions, *J Vac Sci Technol, 17* (1980) 182–185
32 R V Bucur, V Mecea and T B Flanagan, The kinetics of hydrogen (deuterium) sorption by thin palladium layers studied with a piezoelectric quartz crystal microbalance, *Surf Sci, 54* (1976) 477–488
33 R V Bucur and V Mecea, Equilibrium measurements on thin Pd–H layers, *Surf Technol, 11* (1980) 305–322
34 F A Lewis, *The Palladium–Hydrogen System,* Academic Press, London, 1967, p 47
35 A W Warner and C D Stockbridge, Mass measurements with resonating crystalline quartz, in K H Behrndt (ed), *Vacuum Microbalance Technique,* Plenum Press, New York, 1963, pp 55–73
36 R V Bucur and T B Flanagan, The effect of the absorption of hydrogen and deuterium on the frequency of a quartz–palladium resonator, *Z Phys -Chem Neue Folge, 88* (1974) 225–241
37 A Warner, Microweighing with the quartz crystal oscillator, in S P Wolsky and E J Zdanuk (eds), *Ultra Micro Weight Determination in Controlled Environments,* John Wiley, New York, 1969, pp 231–243
38 C D Hodgman (ed in chief), *Handbook of Chemistry and Physics,* Chemical Rubber Publishing Co, Cleveland, OH, p 2502
39 V Mecea and R V Bucur, A new method for the detection of a dangerous gas in the atmosphere, *Romanian Patent No 76465* (1978)
40 V Mecea and E Tătar, Piezoelectric hydrogen detector, *Romanian Patent No 76466* (1978)
41 V Mecea and P Ghete, Thermocompensated ultrasonic hydrogen detector, *Int J Hydrogen Energy, 9* (1984) 861–864
42 C D Hodgman, (ed in chief), *Handbook of Chemistry and Physics,* Chemical Rubber Publishing Co Cleveland, OH, pp 1927–1929

Biography

Vasile-Mihai Mecea was born in 1948 in Brasov He graduated from the Physics Department of the 'Babes-Bolyai' University of Cluj-Napoca in 1972 He received his Ph D in 1979 on a subject concerning the use of the quartz-crystal microbalance for studies on hydrogen and deuterium interaction with palladium films He is currently working on vibrating quartz sensors and thin-film physics He was also involved in hydrogen storage and detection